Doctoral Dissertation

Studies on surface oxidation of plastics using light-activated chlorine dioxide radical gas

光活性化二酸化塩素ラジカルガスによる

プラスチックの表面酸化に関する研究

YANKUN JIA

July 2020

Graduate School of Engineering

Osaka University

Contents

Chapter 3

Surface modification of polycarbonate using the light-activated chlorine dioxide radical

General Introduction

Nowadays, traditional materials, such as metals, glass, and ceramics, are gradually replaced by polymers because of their good behavior in the bulk properties such as resistance to thermal deterioration and chemicals, and intact post-treatment mechanical strength. Besides, their low cost and ease of manufacture also provide a convenience to obtain them, by which polymer products are used in various fields in our daily life. With a broad range of chemical and physical properties for different families of polymeric materials, it is easier to choose polymers for each individual application. Determined by the biocompatibility, biomaterials are commonly used in medical devices such as the syringes[1] and drug delivery systems with the combination of targeting molecules and human tissue implants namely synthetic skin, synthetic blood vessels, artificial hearts, cardiac pacemakers, bone implants.[2,3] Polymers also play an important role in the food packaging industry instead of the traditional material such as glass (heavy and fragile) and paper (high cost and waste). To solve the problem of the depletion of fossil fuels and the corresponding environmental concerns, polymers were also used as a new type of electric energy generator (**Figure 1**).[4,5] Furthermore, the polymer membrane was also used in the water desalination. Therefore, polymers have played an essential role in advancement of technology, applied engineering, and materials.

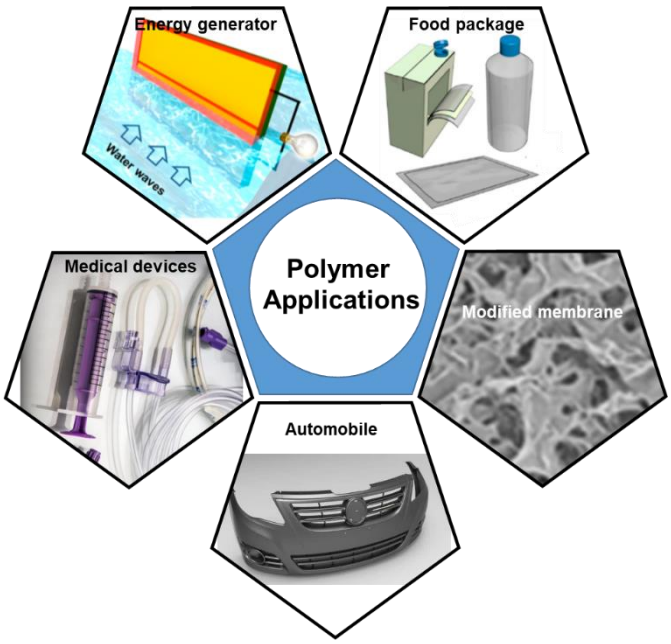

Figure 1. Five examples of polymer applications.

However, their surface properties are correlated to their bulk properties, and most polymers have inert surfaces under ambient conditions. The surface properties of polymers

inhibit their intended wide range of applications and therefore need modification *via* various routes. It would be interesting to tailor the surface properties of a polymer independent of its structure and bulk properties. The researchers are devoted to the development of the techniques to tune their surface properties for the extensive use of polymers. For example, polymer textile materials can be used for the enhancement of neural cell growth rate *via* the modification of their biological cell compatibility by ion implantation.[6] The technique of nanostructured surfaces with functional coatings and generation or release of antimicrobial compounds were used to reduce the interaction of bacteria and microbes with synthetic surfaces in the tissue implants.[7] Many efforts were also performed to adjust the barrier, mechanical, and adhesion properties of the food package polymers such as polyethylene (PE) and polyethylene terephthalate (PET) to meet various requirements.[8,9] To enhance the polymer membrane resistance, the researchers controlled the membrane fouling through layer-by-layer assembly.[10] Surface modification of polymers is widely used to impart desirable properties to a specific application.

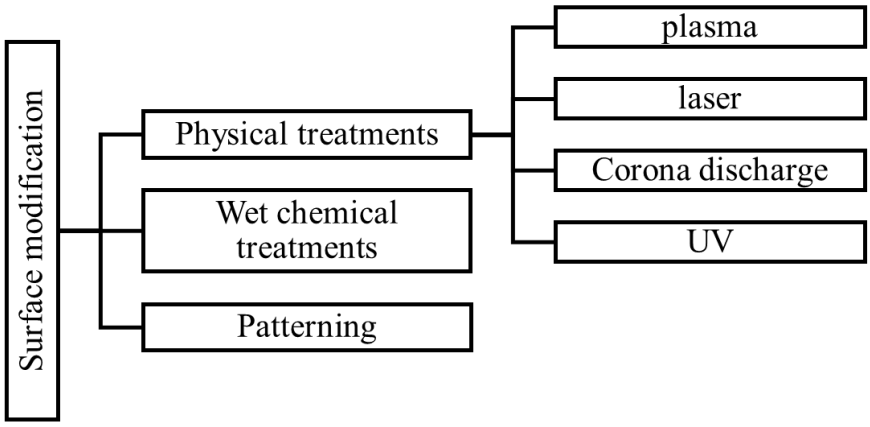

Figure 2. The sorts of polymer surface modification methods.

In general, the surface modification of polymer substrates can be achieved *via* two strategies: 1) to modulate the surface energy of polymer material. The surface hydrophilicity, adhesion property, surface absorbing and releasing are achieved by the addition of functional groups onto the polymer surface. 2) mechanical anchorage owing to the high roughness or

porosity of the plastic surface. The surface modification methods are always classified into physical treatment, wet chemical treatment and patterning (**Figure 2**).

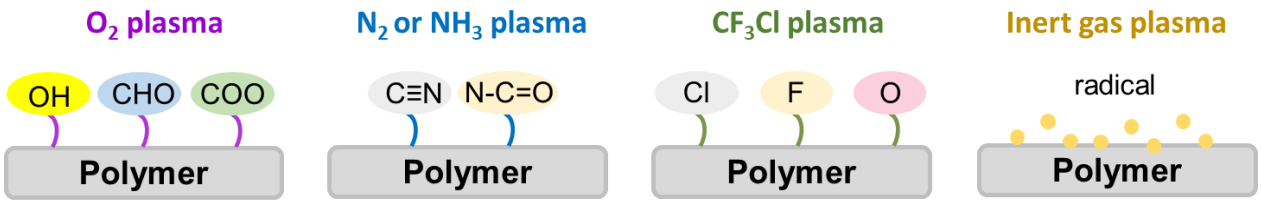

Figure 3. Different functional groups are introduced on the polymer surface basing on the nature of the process gas.

Physical treatments such as plasma, laser and corona discharge are considered to be a clean and fast process without addition of other unwanted elements. Among the physical treatments, plasma is a widely accepted route that can be used in the surface of most types of polymer materials. According to the nature of the process gas (**Figure 3**), the numerous approaches that have been developed for the plasma treatment can be divided into two types that used reactive or inert gas.[11] With the reactive gas, the functional groups can be directly introduced into polymer material surface by the plasma treatment. For instance, plasma treatment using air or oxygen introduced the oxygen-containing groups such as C–O, C=O and O–C=O onto the surfaces of polypropylene (PP)[12,13], polycarbonate (PC)[14], poly (ethylene terephthalate) (PET)[15], acrylonitrile butadiene styrene (ABS)[16], polystyrene (PS)[17] and also specific polyester nonwoven fabrics[18]. Carboxylate groups on PP[19] and PC[20] were reported to be generated by plasma treatment with CO_2 gas. C–N, N–C=O, and possibly C=N has been confirmed to be incorporated into the PC surface by plasma treatment with N_2 or NH_3.[21,22] H_2O gas was also applied in the plasma treatment to introduce the oxygen containing groups to PC, PET[23] and polyethylene (PE), PS, PP[24]. The N and O containing groups can also be incorporated onto PC surface by atmospheric plasma at the same time.[25] Besides, the incorporation of Cl, F, and O was observed on PP treated under the specific CF_3Cl plasma.[26] For the second type, inert gas plasma is used to generate free radicals subsequently using them

in a grafting procedure.[27–30] Plasma treatment not only provides chemical bonding but also has effect on the roughness of polymers surfaces. However, the polar functional groups induced *via* plasma treatment suffer from rotation and migration in the days following the treatment and the hydrophilicity cannot keep stable.[31,32] Besides, the plasma treatment requires for high energy and expensive equipment.

Another physical treatment using laser has also been utilized for surface modification of many types of materials including plastics and various applications. For instance, the PET foil surface was immobilized with silver nanoparticles by the action of polarized excimer laser light for its antibacterial property.[33] Wilhelm Pflegin and coworkers have developed a laser-assisted modification of PS to obtain a chemically modified PS surface bearing carboxylic acid groups well-suited for controlled competitive protein adsorption or protein immobilization.[34] Polyamide fabric has been treated under CO_2 laser to improve the dyeability of fabric.[35] The surface modification of fluorocarbon polymer films was carried out with ArF excimer laser irradiation and selective-area electroless plating of nickel metal on the surface has been achieved.[36] Besides, the laser induced chemical and physical modification has been reported to be associated with the irradiation wavelength.[37] Surface modification using a laser can be carried out in different ways such as etching, ablation, evaporation, surface functionalization, etc. Laser beams can be precisely directed onto designate location even from long distances without losing energy and easy to control. However, the capital investment and operational costs of laser surface treatments are still high. Thermal properties are also limited because of the possibility of thermal damage.[38]

Other physical treatment has also been utilized for modification of polymers surface to modulate their surface properties for different purposes. Corona discharge could modify the polymer surface by rearranging free radicals on the surface to form functional groups that directly enhance hydrophilicity and adhesion.[39] Corona discharge modification on the PP[40,41] and low density PE[42,43] and the subsequent effect on adhesion property have been studied. Recently, corona discharge treatment has been employed for the modification of fibers to improve the dyeability[44,45] and interfacial compatibility[46]. Besides, the surface properties after

corona discharge modification can also be modulated by controlling the operating conditions such as temperature[47]. UV treatment is also an effective, economical and an efficient noncontact polymer surface modification method, which is usually performed on photopolymers. The UV light initiates a photochemical reaction that generates a cross-linked network of polymers along with a change in surface chemical properties like hydrophilicity and adhesion property. The UV induced modification is also based on the generation of radicals on the polymer surface placed in the inert or reactive atmosphere and the possible reactions are shown in **Table 1**.[48] Simultaneously, surface roughness is also increased after UV treatment and can be controlled by the UV irradiation time and wavelength.[49] Moreover, UV-ozone system, which includes an ozone generating device and the UV light source, was designed for the modification of the polymers surfaces.[50–53] This system occurs through insertion of an O (1d) atom to form ether linkages, and hydrogen abstraction by O (3p) to form carbonyl and/or carboxyl functional groups, which is more efficient for surface energy improvement. Besides, another function of UV in the surface modification is used as an inducer to achieve functional grafting with organic molecules.[54,55]

Table 1. Possible reactions following UV-lamp irradiation.

Type	Scheme	Effect
1.Recombination	$A_1^* + {}^*A_1 \rightarrow A_1\text{-}A_1$	None
2.Reaction with radical(s) of a neighboring chain	$A_1^* + {}^*A_2 \rightarrow A_1\text{-}A_2$	Crosslinking
3.Reaction with reactive atmosphere	$A_1^* + Z \rightarrow A_1\text{-}Z^*$	Addition
4.Reaction with bi-functional substance	$A_1\text{-}Z^* + {}^*A_2 \rightarrow A_1\text{-}Z\text{-}A_2$	Crosslinking, thin layer deposition

Apart from the physical treatments mentioned above, wet chemical treatment is also an important approach for surface modification to obtain a surface with the aimed functional groups and subsequent properties. Especially, the wet chemical grafting is suitable for bio-application, for example, the improvement of adhesion with cell on the polymers[56,57] or antibacterial property[58–60] *via* grafting the corresponding compounds. Besides, the wet chemical modification can also improve the metal adhesion to the polymer surfaces.[61,62] while

wet chemical treatments provide a wide range of reagents to selectively treat polymers at large scale, they require a harsh approach with the precise strength of the reagent and the time of treatment. Moreover, additional procedures may generate the hazardous waste. In practical application, physical and chemical treatments are usually combined for the easier operation and better property. For example, plasma treated polypropylene was surface-modified with polydopamine (PDA) in an aqueous medium without employing other chemicals.[63]

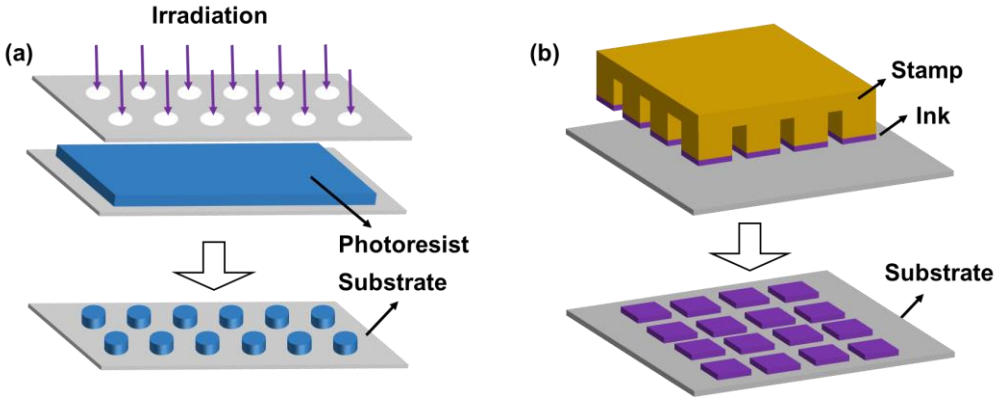

Figure 4. Schemes of process of (a) photolithography and (b) one sort of printing.

In addition, except of the introduction of the functional groups, polymer surface properties and their applications can also be adjusted by the surface patterning. Surface patterning of polymers is an indispensable approach for research fields including cell biology, tissue engineering and medicinal science and the development of optics and electronics. For example, the cells have been patterned on the PDA-micropatterned substrates through selective adhesion to the PDA-coated region.[64] Daniel Zabetakis and Walter J. Dressick used the top-surface imaging and hybrid photoresist/self-assembled monolayer patterning approaches, in conjunction with selective electroless metal deposition, to develop processes capable of fabricating appropriate submicron and nanoscale metal features useful as electrical interconnects.[65] Zhihong Nie and Eugenia Kumacheva[66] have summarized the techniques for the surface patterning, including photolithography and printing (**Figure 4**). Besides, interface

wrinkle whose orientation and geometry can be tailored plays a distinguishing role for the surface patterning.[67,68]

Although the surface modification methods of polymers have been developed for years, all the methods have merits and defects. The study and development on mild and highly effective polymers surface modification is still in high demand. Previously, the oxidation of methane to methanol and formic acid has been achieved by a recently proposed novel method using light-activated chlorine dioxide radical ($ClO_2^{\bullet}$).[69] Photochemical oxygenation of methane occurred in a two-phase system under ambient conditions. The methanol and formic acid were highly yielded with a methane conversion of 99% without formation of the further oxygenated products such as CO_2 and CO. In this oxidation, the chlorine radical ($Cl^{\bullet}$) generated from the $ClO_2^{\bullet}$ upon light activation cleaved the C-H bond, and the subsequent addition of singlet oxygen provided an oxygenated product (**Figure 5**). Upon this reaction mechanism, this oxidation using light-activated $ClO_2^{\bullet}$ was supposed to be applied as a surface modification strategy for polymer chain.

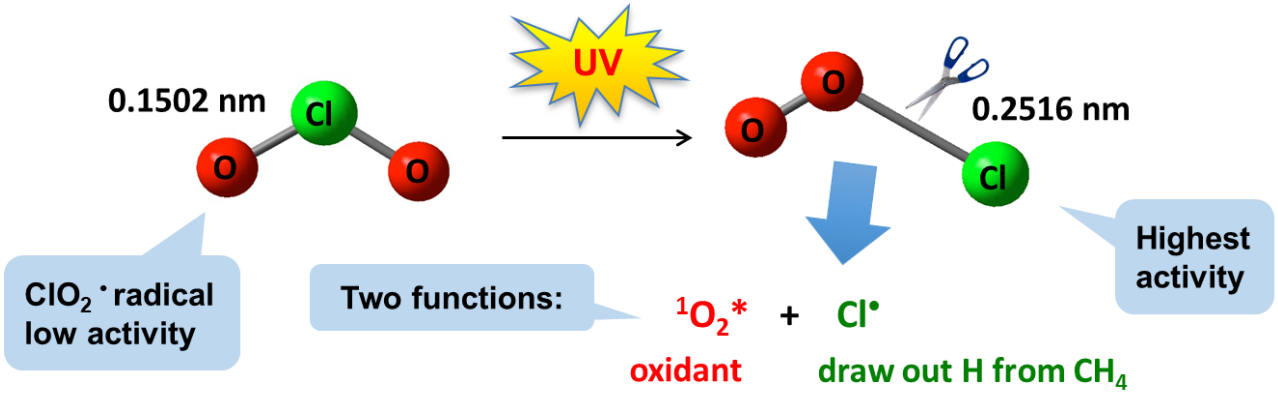

Figure 5. The functions of $ClO_2^{\bullet}$ under the light irradiation.

On the other hand, the metallization of polymer is the most attractive and applied in a large variety of technological applications. Polymers are always considered as alternatives to conventional metal-based devices. For example, the metallized polymer can be used in the automobile industry as a component of automobile, such as bumper, to reduce its weight to improve the fuel efficiency. After metallization, polymers can also be applied as the substrate

in the fabrication of printed circuits in microelectronics, which possess the toughness, torsion resistance and light weight. With the progress of the times and the development of technology, the higher demand for decorative coating material also require the metallization of polymers. For instance, the adhesion of sputtered Cu films on UV-ozone modified poly (methyl methacrylate) (PMMA) substrates was enhanced *via* UV-ozone treatment, based on which, a 6-in. PMMA chip with arrays of three-electrode electrochemical microsensors was designed and fabricated (**Figure 6**).[70] There are two sorts of metallization of plastics: one is direct adhesion between polymer and metal foil or plate using an adhesive. Most of adhesives are regarded as contaminations due to the toxic components. To reduce the use of toxic substance and simply the operations, adhesive-free adhesion is desired. To date, few studies about adhesive-free adhesion between polymer and metal has been reported. Polydimethylsiloxane (PDMS) surface was successfully adhered to hard metal material *via* plasma treatment.[71,72] PP surface grafted with maleic anhydride showed good adhesion with Cu without adhesive, which can be utilized as a coating for copper wires and cables.[73] The other type of metallization of polymer is metal plating on polymer surface. Metal plating includes electroplating and electroless plating. Compared with electroplating, the metal deposition on the electroless plated polymer surface was more uniform. The surface conductivity and specific shape of polymer were not required. Therefore, the electroless plating was widely applied. However, for the electroless plating, adhesion and film quality improvement and ability of plating for complex shapes are still desired, which is based on surface modification. For example, high-resolution and well-defined metallic circuits fabricated *via* electroless Cu plating were successfully prepared on the polymer surface by laser direct structuring.[74]

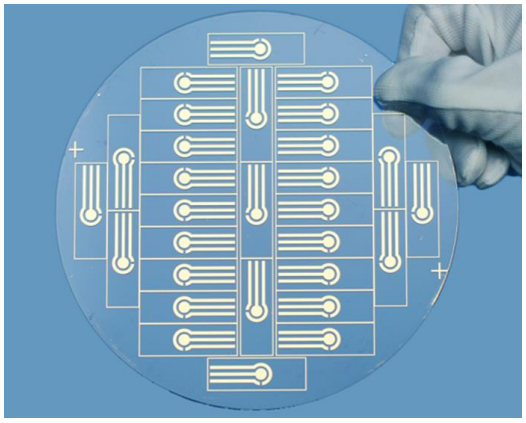

Figure 6. The picture of electrochemical microsensors fabricated *via* the adhesion of sputtered Cu films on UV-ozone modified PMMA substrate.

Furthermore, three types of engineering plastics, polypropylene (PP), acrylonitrile butadiene styrene (ABS) and polycarbonate (PC), are chosen for investigation. These three types of engineering plastics have their own specific chemical structures and properties and have been practically used for different purposes. PP is produced *via* chain-growth polymerization from the monomer propylene, belonging to the group of polyolefins and is partially crystalline and non-polar. PP is a commodity plastic with properties of high wear resistance and torsion resistance, which can be used in textile, package, food industry, coating fields. Considering the chemical structure, PP is a simple alkane with methyl groups in the side chains. ABS is a terpolymer made by polymerizing styrene and acrylonitrile in the presence of polybutadiene. The ratio of the three monomers can be modulated. ABS is amorphous and therefore has no true melting point. It possesses the characters of high strength, high toughness and ease of processing. Due to the uniformly distributed butadiene, ABS is usually considered as the best choice for electroless metal plating. Besides, it has also been utilized for the fabrication of musical instruments, luggage, automotive components and Lego. Polycarbonates used in engineering are strong, tough materials, and some grades are optically transparent, so they are widely used for manufacturing CD, lens, water bottle, and bulletproof glass. Considering the chemical structure, PC has an oxygen containing structure, and the aromatic carbons exist in its main chain while methyl groups in the side chain. Despite of the differences, the common character for them is low surface energy and poor adhesion property with heterogeneous materials.

Therefore, in this thesis, the surfaces of the three types of engineering plastics, were modified via the oxidation using light-activated $ClO_2^{\bullet}$ mentioned before. Subsequently, the adhesions of three plastics with metal material were also evaluated (**Figure 7**).

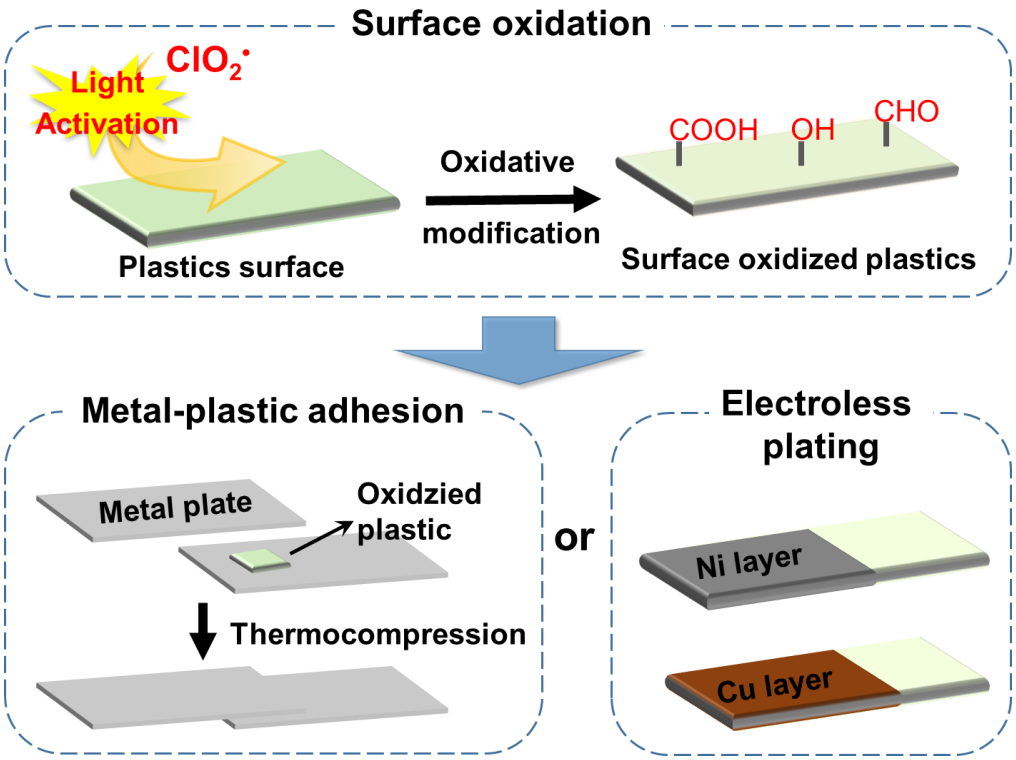

Figure 7. The scheme of the oxidation of three plastics and the subsequent adhesion evaluations in this thesis.

Contents of this thesis

Chapter 1

In this chapter, PP film surface was modified by the recently proposed oxidation method using light-activated $ClO_2^{\bullet}$ gas. The surface chemical compositions, hydrophilicity and adhesion behavior with metal were studied. The effects of oxidation conditions on oxidation degree and oxidation depth and the effect of oxidation temperature on the adhesion strength with Al plate were further investigated. Moreover, this chapter developed an approach for the electroless metal plating on PP surface. The influence of light irradiation on the activation of $ClO_2^{\bullet}$ and modification process was studied and light irradiation was found that only required to activate $ClO_2^{\bullet}$ gas but have no direct modification on PP, by which the internal void could be oxidized and electroless plating for a complicated structure was possible.

Chapter 2

In this chapter, the modification method *via* oxidation using light-activated $ClO_2^{\bullet}$ was used to oxidize the surface of ABS resin. The surface chemical composition, hydrophilicity and surface morphology were investigated. As a result, butadiene in the ABS resin was confirmed to be oxidized. The adhesion of the metal layer deposited on the oxidized ABS resin after electroless plating was also studied. Furthermore, the effects of different oxidation time and temperatures on the chemical composition, hydrophilicity and adhesion were investigated to obtain optimal conditions. This chapter aims to develop an environmentally friendly and efficient way to modify ABS resin surface which can be applied for further electroless metal plating.

Chapter 3

In this chapter, $ClO_2^{\bullet}$ was used as an oxidizing agent for PC oxidation by light irradiation under ambient conditions. The chemical composition, hydrophilicity and transparency of the PC film surface after oxidation were analyzed. The effects of the oxidation conditions, viz. temperature and time, were also investigated. The oxidized PC films were subjected to electroless plating. This research aims to achieve the surface modification of PC *via* oxidation for the further modification or application.

References

1. W. Brostow, D. Pietkiewicz and S. R. Wisner, *Adv. Polym. Technol.*, 2007, **26**, 56–64.
2. N. P. Tipnis and D. J. Burgess, *Int. J. Pharm.*, 2018, **544**, 455–460.
3. D. F. Williams, *Journal of Materials Science*, 1987, **22**, 3421–3445.
4. T. Xu, X. Ding, Y. Huang, C. Shao, L. Song, X. Gao, Z. Zhang and L. Qu, *Energy Environ. Sci.*, 2019, **12**, 972-978.
5. G. Zhu, Y. Su, P. Bai, J. Chen, Q. Jing, W. Yang and Z. L. Wang, *ACS Nano* 2014, **8**, 6031–6037.
6. A. G. Nikolaev, G. Y. Yushkov, E. M. Oks, A. Oztarhan, A. Akpek, E. Hames-Kocabas, E. S. Urkac and I. G. Brown, *Appl. Surf. Sci.*, 2014, **310**, 51–55.
7. S. Rigo, C. Cai, G. Gunkel-Grabole, L. Maurizi, X. Zhang, J. Xu and C. G. Palivan, *Adv. Sci.*, 2018, **5**, 1700892.
8. M. Ozdemir, C. U. Yurteri and H. Sadikoglu, *Crit. Rev. Food Sci. Nutr.*, 1999, **39**, 457–477.
9. C. Vasile, *Materials*, 2018, **11**, 1834.
10. J. Saqib and I. H. Aljundi, *J. Water Process Eng.*, 2016, **11**, 68–87.
11. F. Khelifa, S. Ershov, Y. Habibi, R. Snyders and P. Dubois, *Chem. Rev.*, 2016, **116**, 3975–4005.
12. O.-J. Kwon, S. Tang, S.-W. Myung, N. Lu, H.-S. Choi, *Surf. Coatings Technol.*, 2005, **192**, 1–10.
13. R. Morent, N. De Geyter, C. Leys, L. Gengembre and E. Payen, *Surf. Interface Anal.*, 2008, **40**, 597–600.
14. T. G. Shikova, A. A. Ovtsyn and S. A. Smirnov, *High Energy Chem.*, 2019, **53**, 326–330.
15. J. Friedrich, I. Loeschcke, H. Frommelt, H. D. Reiner, H. Zimmermann and P. Lutgen, *Polym. Degrad. Stab.*, 1991, **31**, 97–114.
16. J. Abenojar, R. Torregrosa-Coque, M. A. Martínez and J. M. Martín-Martínez, *Surf. Coatings Technol.*, 2009, **203**, 2173–2180.
17. A. Vesel, *Surf. Coatings Technol.*, 2010, **205**, 490–497.

18. M. Šimor, J. Ráhel', M. Černák, Y. Imahori, M. Štefečka and M. Kando, *Surf. Coatings Technol.*, 2003, **172**, 1–6.
19. G. qiu Ma, X. ning Liu, D. hai Huang, X. bo Yuan and J. Sheng, *Appl. Surf. Sci.*, 2009, **255**, 7483–7494.
20. A. Moustaghfir, E. Tomasella, M. Jacquet, A. Rivaton, B. Mailhot, J. L. Gardette and E. Bêche, *Thin Solid Films*, 2006, **515**, 662–665.
21. A. Laskarakis, S. Kassavetis, C. Gravalidis and S. Logothetidis, *Nucl. Instruments Methods Phys. Res. Sect. B Beam Interact. with Mater. Atoms*, 2010, **268**, 460–465.
22. T. Sato, H. Akiyama, S. Horiuchi and T. Miyamae, *Surf. Sci.*, 2018, **677**, 93–98.
23. B. D. Tompkins, J. M. Dennison and E. R. Fisher, *J. Memb. Sci.*, 2013, **428**, 576–588.
24. B. D. Tompkins and E. R. Fisher, *J. Appl. Polym. Sci.*, 2015, **132**, 41978.
25. H. Yaghoubi and N. Taghavinia, *Appl. Surf. Sci.*, 2011, **257**, 9836–9839.
26. S. Corn, K. P. Vora, M. Strobel and C. S. Lyons, *J. Adhes. Sci. Technol.*, 1991, **5**, 239–245.
27. C. Wang, J. rong Chen and R. Li, *Appl. Surf. Sci.*, 2008, **254**, 2882–2888.
28. C. Zhang and K. Fang, *Surf. Coatings Technol.*, 2009, **203**, 2058–2063.
29. M. R. Chashmejahanbin, A. Salimi and A. Ershad Langroudi, *Int. J. Adhes. Adhes.*, 2014, **49**, 44–50.
30. V. Švorčík, K. Kolářová, P. Slepička, A. Macková, M. Novotná and V. Hnatowicz, *Polym. Degrad. Stab.*, 2006, **91**, 1219–1225.
31. W. J. Brennan, W. J. Feast, H. S. Munro and S. A. Walker, *Polymer*, 1991, **32**, 1527–1530.
32. R. Sharma, E. Holcomb, S. Trigwell and M. Mazumder, *J. Electrostat.*, 2007, **65**, 269–273.
33. P. Slepička, J. Siegel, O. Lyutakov, N. Slepičková Kasálková, Z. Kolská, L. Bačáková and V. Švorčík, *Biotechnol. Adv.*, 2018, **36**, 839–855.
34. W. Pfleging, M. Torge, M. Bruns, V. Trouillet, A. Welle and S. Wilson, *Appl. Surf. Sci.*, 2009, **255**, 5453–5457.
35. M. I. Bahtiyari, *Opt. Laser Technol.*, 2011, **43**, 114–118.
36. H. Niino and A. Yabe, *Appl. Phys. Lett.*, 1993, **63**, 3527–3529.
37. T. Lippert, T. Nakamura, H. Niino and A. Yabe, *Appl. Surf. Sci.*, 1997, **109**, 227–231.

38. M. Ozdemir and H. Sadikoglu, *Trends Food Sci. Technol.*, 1998, **9**, 159–167.

39. J. F. Carley and P. T. Kitze, *Polymer Engneering and Science*, 1980, **20**, 330–338.

40. M. Strobel and C. S. Lyons, *J. Adhes. Sci. Technol.*, 2003, **17**, 15–23.

41. M. Strobel, C. Dunatov, J. M. Strobel, C. S. Lyons, S. J. Perron and M. C. Morgen, *J. Adhes. Sci. Technol.*, 1989, **3**, 321–335.

42. S. J. Park and J. S. Jin, *J. Colloid Interface Sci.*, 2001, **236**, 155–160.

43. I. Novák and Š. Florián, *Macromol. Mater. Eng.*, 2004, **289**, 269–274.

44. M. P. Gashti, I. Ebrahimi and M. Pousti, *Curr. Appl. Phys.*, 2015, **15**, 1075–1083.

45. N. Ristic´, P. Jovancˇic´, C. Canal, D. Jocic´, *J. Appl. Polym. Sci.*, 2010, **117**, 2487–2496.

46. M. Ragoubi, B. George, S. Molina, D. Bienaimé, A. Merlin, J. M. Hiver and A. Dahoun, *Compos. Part A Appl. Sci. Manuf.*, 2012, **43**, 675–685.

47. P. Ma, J. Huang, G. Cao and W. Xu, *Fibers Polym.*, 2010, **11**, 941–945.

48. S. L. Gao, R. Häler, E. Mäder, T. Bahners, K. Opwis and E. Schollmeyer, *Appl. Phys. B Lasers Opt.*, 2005, **81**, 681–690.

49. W. Chen, J. Zhang, Q. Fang, K. Hu and I. W. Boyd, *Thin Solid Films*, 2004, **453**–**454**, 3–6.

50. L. F. Macmanus, M. J. Walzak and N. S. Mcintyre, *J. Polym. Sci. Part A Polym. Chem.*, 1999, **37**, 2489–2501.

51. B. Gongjian, W. Yunxuan and H. Xingzhou, *J. Appl. Polym. Sci.*, 1996, **60**, 2397–2402.

52. R. O. F. Verkuijlen, M. H. A. Van Dongen, A. A. E. Stevens, J. Van Geldrop and J. P. C. Bernards, *Appl. Surf. Sci.*, 2014, **290**, 381–387.

53. A. S. Bhurke, P. A. Askeland and L. T. Drzal, *J. Adhes.*, 2007, **83**, 43–66.

54. S. Hu, X. Ren, M. Bachman, C. E. Sims, G. P. Li and N. Allbritton, *Anal. Chem.*, 2002, **74**, 4117–4123.

55. D. E. Weibel, A. F. Michels, F. Horowitz, R. da Silva Cavalheiro and G. V. da Silva Mota, *Thin Solid Films*, 2009, **517**, 5489–5495.

56. C. Löhbach, U. Bakowsky, C. Kneuer, D. Jahn, T. Graeter, H. J. Schäfers and C. M. Lehr, *Chem. Commun.*, 2002, **21**, 2568–2569.

57. M. Gabriel, K. Niederer, M. Becker, C. M. Raynaud, C. F. Vahl and H. Frey, *Bioconjug. Chem.*, 2016, **27**, 1216–1221.

58. M. Kazemi Ashtiani, M. Zandi, P. Shokrollahi, M. Ehsani and H. Baharvand, *Polym. Adv. Technol.*, 2018, **29**, 1227–1233.

59. S. Swar, V. Zajícová, M. Rysová, I. Lovětinská-Šlamborová, L. Voleský and I. Stibor, *J. Appl. Polym. Sci.*, 2017, **134**, 1–11.

60. M. Herrero, R. Navarro, Y. Grohens, H. Reinecke and C. Mijangos, *Polym. Degrad. Stab.*, 2006, **91**, 1915–1918.

61. S. Siau, A. Vervaet, E. Schacht, U. Demeter and A. Van Calster, *Thin Solid Films*, 2006, **495**, 348–356.

62. K. W. Lee and A. Viehbeck, *IBM J. Res. Dev.*, 1994, **38**, 457–474.

63. V. K. Thakur, D. Vennerberg and M. R. Kessler, *ACS Appl. Mater. Interfaces*, 2014, **6**, 9349–9356.

64. S. H. Ku, J. S. Lee and C. B. Park, *Langmuir*, 2010, **26**, 15104–15108.

65. D. Zabetakis and W. J. Dressick, *ACS Appl. Mater. Interfaces*, 2009, **1**, 4–25.

66. Z. Nie and E. Kumacheva, *Nature Materials*, 2008, **7**, 277–290.

67. A. Schweikart and A. Fery, *Microchim. Acta*, 2009, **165**, 249–263.

68. J. Rodríguez-Hernández, *Prog. Polym. Sci.*, 2015, **42**, 1–41.

69. K. Ohkubo and K. Hirose, *Angew. Chemie - Int. Ed.*, 2018, **57**, 2126–2129.

70. J. Liu, L. He, L. Wang, Y. Man, L. Huang, Z. Xu, D. Ge, J. Li, C. Liu and L. Wang, *ACS Appl. Mater. Interfaces*, 2016, **8**, 30576–30582.

71. V. Sunkara, D. K. Park and Y. K. Cho, *RSC Adv.*, 2012, **2**, 9066–9070.

72. R. W. R. L. Gajasinghe, S. U. Senveli, S. Rawal, A. Williams, A. Zheng, R. H. Datar, R. J. Cote and O. Tigli, *J. Micromech. Microeng.*, 2014, **24**, 075010.

73. J. Hrbacek, R. H. Pahler, W. Brostow, A. Hull, I. K. Chen, A. Srinivasan and N. Hnatchuk, *Polym. Test.*, 2017, **63**, 158–162.

74. J. Zhang, T. Zhou, L. Wen and A. Zhang, *ACS Appl. Mater. Interfaces*, 2016, **8**, 33999–34007.

Chapter 1

Polypropylene (PP) surface oxidation by light-activated chlorine dioxide radical for metal−plastics adhesion

1.1 Introduction

Recently, multi-materialization, the use of various materials at the appropriate places, has attracted much attention due to the development and further functionalization of lightweight materials. As described in the general introduction, the plastic/metal composite materials, which involve adhesion of plastic and metal plate[1] and/or electroless metal plating on plastic, are one of the most significant technologies on account of its light weight, high recyclability, steady physical properties and low production cost. For example, the superior properties of heat resistance, corrosion resistance and high mechanical strength to weight ratio allow PP-metal composites to be widely used in various fields, such as automotive, electronics, and packaging.[2-5] In general, however, due to the low adhesion strength of non-polar PP to hydrophilic metals, it is necessary to modify PP surfaces to increase the surface energy without any changes in their bulk properties.

Therefore, both physical and chemical surface treatments of PP have been well developed to improve its adhesive properties.[6,7] Several surface modification methods have been employed, such as corona discharge, plasma treatment and chemical wet oxidation.[8] In the case of corona discharge, oxygen containing groups are effectively introduced in a single step, but the introduced oxygen functional groups are generally unstable and decrease over time.[9,10] In addition, atomic oxygen in the discharge method causes PP chain scission.[11] Although plasma treatment is most commonly used in the industry as a safe and effective method, it could result in cross-linking on the plasma treated layer. In addition, it is difficult to modify all surface area on PP with complicated structures and shapes. Chemical wet oxidation uses strong oxidant and is generally effective as well, but these oxidants are toxic and have disadvantage for the

production of hazardous chemical wastes. Consequently, the development of a safe and simple method with low cost to improve the adhesion property of PP is still highly demanded.

Therefore, according to the oxidation using $ClO_2^{\bullet}$ mentioned in the general introduction, this chapter demonstrated surface oxidation of PP film surface and the adhesive-free adhesion between aluminium and oxidized PP modified by $ClO_2^{\bullet}$ gas with UV irradiation. Oxidation of PP enhanced adhesive property of PP with aluminum. The effects of reaction time and temperature on the oxidation degree, oxidation depth, chemical composition, and adhesive strength were investigated. As a result, it is found that the adhesion strength increased by the increase of oxidation temperature of PP. In addition, XPS measurement revealed that the higher reaction temperature resulted in deeper oxidation depth.

On the other hand, as mentioned in the general introduction, electroless metal plating on plastics is also an important approach in metallization. It is known that PP is one of the most difficult substrates to apply electroless metal plating. Therefore, efficient pre-treatments are needed to improve surface adhesion. Many methods have been developed for surface activation of polymers, such as plasma[12-15], UV[16], layer-by-layer coating[17], chemical etching[18] and grafting for Pd-free plating on the surface[19]. In addition, Takeyasu *et al*., reported an electroless plating method that is useful for metal deposition onto internal obscured regions of a complex structure.[20] Herein, the electroless plating of PP was also investigated *via* modification by light activated $ClO_2^{\bullet}$ oxidation as pre-treatment and this method was also employed onto other polymers with similar chemical structure. In addition, as an important finding, it is found that UV irradiation is only required for the activation of $ClO_2^{\bullet}$ but is unnecessary for the surface of polymer.

1.2 Experimental section

Materials

Sodium chlorite ($NaClO_2$) was commercially obtained from Sigma-Aldrich (Tokyo, Japan). Ni plating reagents ($SnCl_2$, $PdCl_2$, $Ni_2SO_4 \cdot 6H_2O$, Glycine and $NaH_2PO_2 \cdot H_2O$) were

purchased from Nacalai Tesque (Kyoto, Japan). Cu plating solutions (OPC-50 inducer M, OPC-150 Crystal RW, and ATS Addcopper IW) were obtained from Okuno Chemical Industry (Osaka, Japan). The commercial polypropylene (PP) pellets (Prime Polymer, F327) were hot-pressed for 15 min at 175 °C under 10 MPa into films with a thickness of 200 μm. Al plate was purchased from the Nilaco Corporation (Tokyo, Japan) and washed with ethanol before use. PVC (Poly (vinyl chloride)) and PE (Polyethylene) films were purchased from AS ONE Corporation (Osaka, Japan).

Modification of PP film surface

$ClO_2^{\bullet}$ treatment: PP film was oxidized by the $ClO_2^{\bullet}$ gas generated from aqueous solution (7 ml) of $NaClO_2$ (100 mg) and 35% HCl aq. (100 μL) under irradiation with a 60 W LED lamp (λ = 365 nm, 20 mW/cm^2). A new glassware system was devised to perform the oxidation of a PP film in larger size and/or heating condition. The aqueous solution of $NaClO_2$ was filled into outer moat part of glassware and the PP sample was put into inner side. Before the oxidation, the PP film was washed by water and was dried in vacuum drying oven. Plasma treatment: PP film was treated for a minute with a vacuum plasma equipment (Sakigake-Semiconductor, YHS-R).

Surface characterization

The chemical compositions and functional groups were determined by ATR-FTIR (FT/IR4700, JASCO) at room temperature with a diamond window. All spectra were acquired at 4 cm^{-1} resolutions over 100 scans in the scan range of 500–4000 cm^{-1}. To confirm the reproducibility, the measurement was performed over twice for each sample. Elemental compositions of the surface were calculated using X-ray photoelectron spectroscopy (XPS: Kratos Ultra 2). The XPS parameters included the power of analysis (wide: 75 W, narrow: 150 W), monochromatic Al Kα. The survey and high-resolution XPS spectra were collected at fixed analyzer pass energies of 160 eV and 10 eV, respectively. To confirm the reproducibility, the measurement was performed over twice for each sample. Binding energies were referred to C-

H (sp3) carbon for C 1s peak set at 285.0 eV. The peaks were fitted by using CasaXPS Version 2.3.15 computer program (Casa Software Ltd). Static contact angle was determined by using a Drop Master DM300 (Kyowa Interface Science). 1.0 μL of water droplet was fixed onto the surface and the contact angle was determined at 5 sec (scanning time) after the attachment of the droplet. Data are obtained as the mean of five independent experiments with standard deviation.

Adhesion of PP to metal

Adhesion of PP to metal plate was performed by thermocompression bonding without any adhesives. The PP film was cut into 3×3 mm^2 and was placed between two pieces of Al plates, then the thermocompression bonding was carried out at 160 °C under 20 MPa for 5 min. The Al/PP/Al were loaded to failure at 5 mm/min in tensile mode, and the failure strain was measured. Data are obtained as the mean of three independent experiments with standard deviation.

Electroless plating

Ni Plating: the conventional two-step catalyzation, sensitizing/activation method, was applied to deposit the Pd catalyst on PP film. The sensitization was carried out by immersing the film in a mixture of 10 mM $SnCl_2$ and 200 mM HCl aqueous solution for 2 min at room temperature. The activation was carried out by immersing in a mixture of 1 mM $PdCl_2$ and 200 mM HCl aqueous solution for 2 min at room temperature. This sensitizing/activation treatment was repeated twice. Electroless plating was then performed in a solution comprising 100 mM $NiSO_4 \cdot 6H_2O$, 200 mM Glycine, 200 mM $NaH_2PO_2 \cdot H_2O$ and H_2O, pH 5.0, for 20 min at 75 °C. Cu plating: the catalyst loading was achieved by dipping into OPC-50 Inducer M solution at 45 °C for 6 min and then into OPC-150 Crystal RW solution at 25 °C for 5 min. Copper deposition was conducted by immersing in ATS Addcopper IW solution at 25 °C for 1 min. The adhesion of metal layer to polymer film was evaluated through a cross-cut tape adhesion test.

1.3 Results and discussion

Surface modification of polypropylene (PP) by light activated chlorine dioxide radical ($ClO_2^{\bullet}$)

In order to confirm the hydrophobicity of PP surface before and after oxidation, the water contact angle was measured. The untreated PP film showed hydrophobicity with a contact angle of 107±0.9° (**Figure 1-1**a), while the contact angle of PP film oxidized *via* light-activated $ClO_2^{\bullet}$ at 25 °C for 10 min decreased to about 86±1.8° (**Figure 1-1**b).

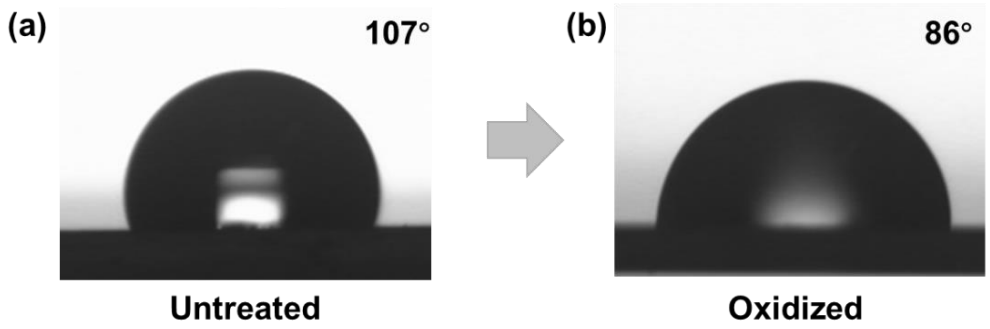

Figure 1-1. Pictures of the water contact angle of (a) the untreated and (b) oxidized PP surface.

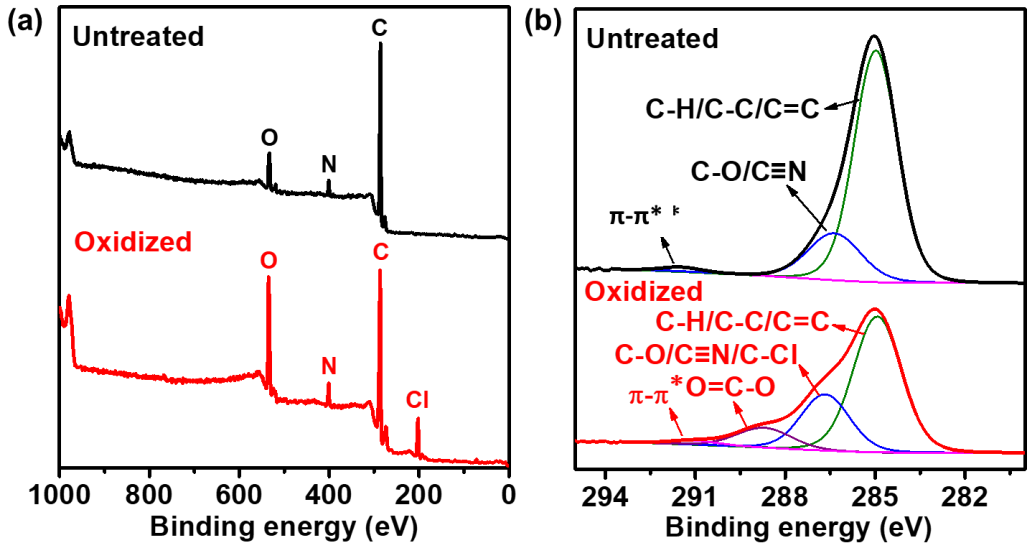

Figure 1-2. (a) XPS wide scan spectra and (b) C1s spectra of untreated PP film surface and oxidized (oxidized at 25 °C for 10 min) PP film surface.

Moreover, to examine the details of introduced functional groups, X-ray photoelectron spectroscopy (XPS) was employed to untreated and oxidized PP films (oxidized at 25 °C for 10 min) (**Figure 1-2**). C1s is the major component on the surface of untreated PP film, while C1s and O1s can be assigned to oxidized PP film. According to **Figure 1-2**a, the results reveal that oxidation leads to a significant increase in oxygen content (3.9% to 15.2%), and small amount of chlorine is incorporated into the surface after oxidation. **Figure 1-2**b shows C1s spectra of PP film before and after oxidation for 10 min at 25 °C respectively. The spectra of untreated PP film reveal the presence of main peak with binding energy about 285.0 eV for C-C/C-H. The oxidized PP film also shows peaks around 285.0 eV, 286.5 eV and 288.0 eV, which are attributed to C-O, C-Cl and O-C=O respectively. The oxidized portion of PP was also studied in our group.[21] PP contains primary C-H bonds in the side chains and secondary and tertiary C-H bonds in the main chain and the bond dissociation energy of these C-H bonds decrease in the order primary, secondary and tertiary one. However, the most feasible reaction for the oxygenation is the O_2-addition to primary carbon to yield the corresponding peroxyl radical and the rate-determining step of oxygenation is the O_2-insertion to form the peroxyl radical group.

The effect of oxidation time on chemical component ratio (**Figure 1-3**a) was investigated to reveal the relationship between reaction condition and oxidation degree. The samples were oxidized at 25 °C at different oxidation time. The chemical component ratio was calculated from the XPS C1s spectra. The sum ratio of oxygen containing functional groups (C-O and COO) was about 35% when the PP film surface was oxidized for 3 min. When the oxidation time was extended to 10 minutes, the ratio of oxygen containing functional groups reached saturation. When the oxidation time was longer than 10 min, no significant difference was found for the amount of oxygen, thus it was decided that the reaction time for oxidation of samples for further studies was 10 min.

The effect of the oxidation temperature (25°C, 60°C and 90°C) on chemical component ratio was also investigated (**Figure 1-3**b). Even when reaction temperature was increased to

60 °C or 90 °C, the sum of the oxygen containing group ratio was around 40%, which is almost as the same as the ratio of reaction at 25 °C.

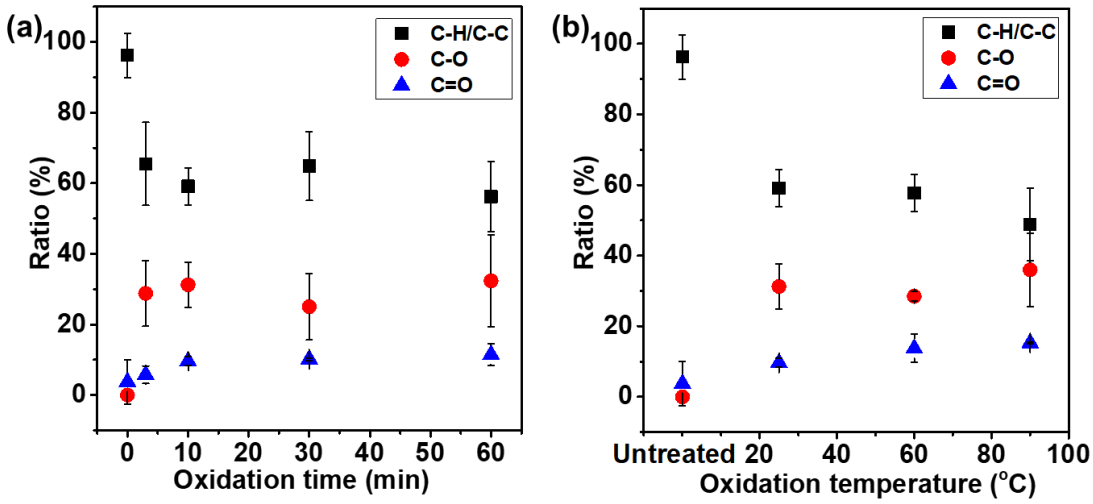

Figure 1-3. (a) The relation curves of oxidation time-chemical components ratio calculated from C1s spectra; (b) The relationship between oxidation temperature and chemical components ratio calculated from C1s spectra. Data are displayed as the mean of three independent experiments with standard deviation.

Adhesion between metal and oxidized PP

The adhesion strength was measured as a function of oxidation temperature (**Figure 1-4**a, b). As shown in **Figure 1-4**c, the adhesion strength became higher as the oxidation temperature of PP raised. From the results of **Figure 1-4**d, the adhesion became stronger with the increase of oxidation degree. As seen from XPS and IR studies, the oxidation created -COOH groups on PP surface. These results indicate that there is the strong interaction between oxygenated functional groups on PP and aluminum surface. The interaction between carboxylate groups of maleic anhydride-modified PP and Al sheet has been reported, which was confirmed to be the reason of interfacial adhesive strength by the electron donor-acceptor interaction.[22,23] Besides, the high surface roughness of the PP film oxidized at high temperature was not considered to be the main reason for the adhesion improvement because the adhesion experiment was conducted by the thermocompression and the PP film surface turned to be smooth after adhesion experiment. Compared to the untreated PP film, with the increase of

oxidation temperature, the adhesion strength of oxidized PP film could reach about 23±2.7 N/mm^2, which was about 7 times higher than that of untreated PP (**Figure 1-4**c). In addition, plasma treatment, which is the most common treatment for PP modification, only led to a maximum adhesion strength of 7±0.5 N/mm^2.

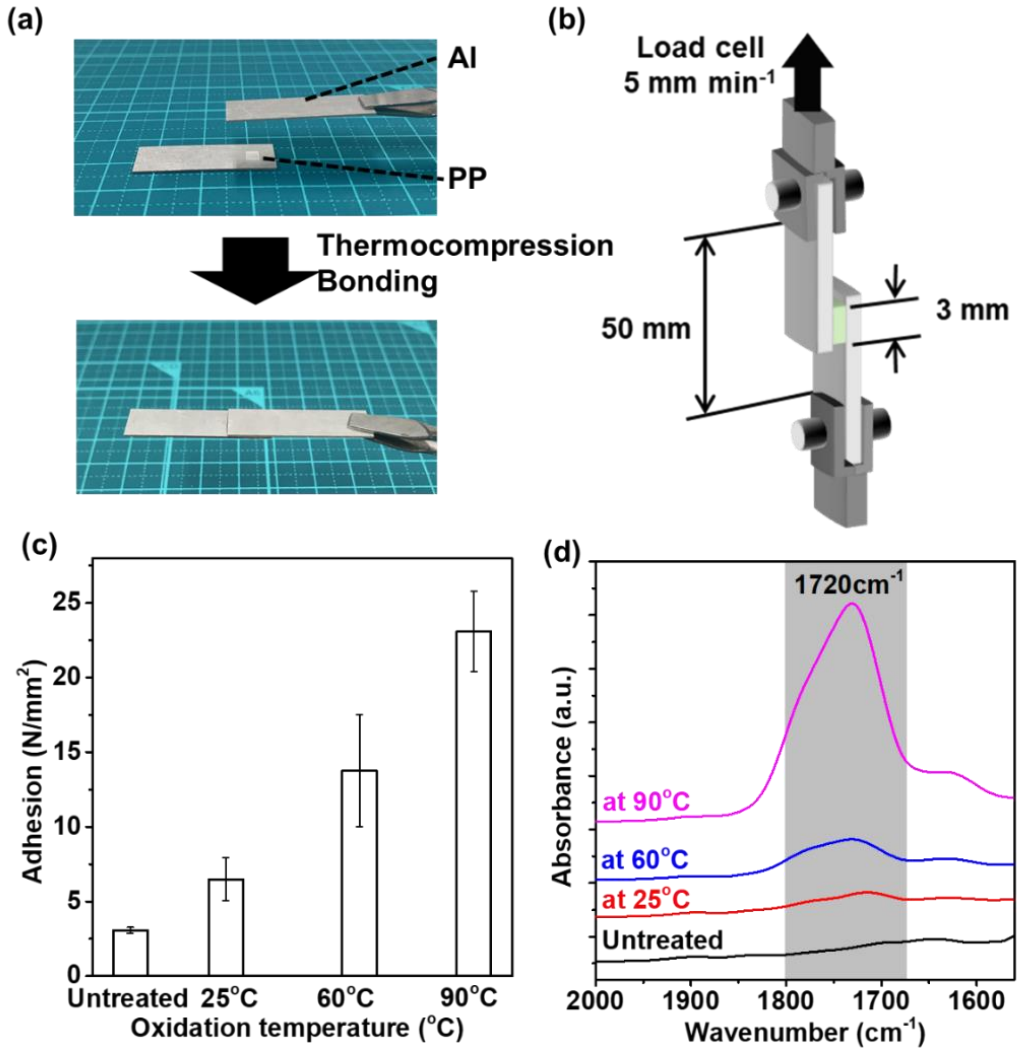

Figure 1-4. (a) Pictures of before and after thermocompression bonding of Al/PP/Al; (b) Schematic illustration of the adhesion strength test; (c) The relationship between adhesion strength and oxidation temperature of untreated PP and PP treated under the UV light with $ClO_2^{\bullet}$; (d) ATR-IR spectra of untreated PP film and PP films oxidized at 25, 60 and 90 °C. Data are displayed as the mean of five independent experiments with standard deviation.

Although there was no significant difference in the ratio of the polar functional groups on the surface of the treated PP film (**Figure 1-3**b), the adhesion strength increased with

increasing oxidation temperature (**Figure 1-4**c). On the other hand, peak intensity at the 1720 cm^{-1} region for IR increased (**Figure 1-4**d), indicating that the increase in adhesion strength could be the result of the incorporation of functional groups in the depth direction at higher oxidation temperature.

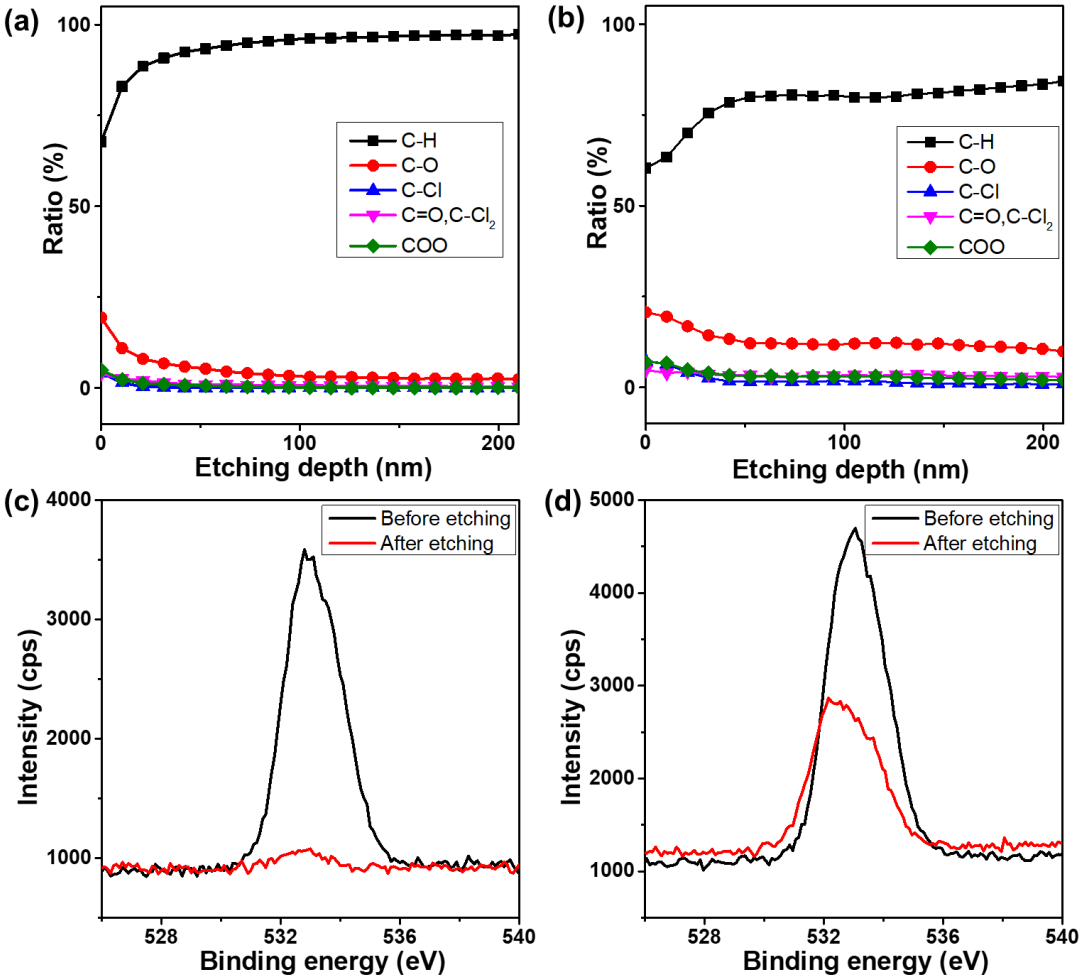

Figure 1-5. (a, b) Chemical composition with the etching depth of PP film oxidized at (a) 25 °C and (b) 90 °C for 10 minutes; (c, d) O1s spectra of PP film before and after 210 nm etching. Oxidation temperatures were (c) 25 and (d) 90 °C, respectively.

To further quantitatively evaluate the depth of oxidation, untreated PP and oxidized PP films were etched by the Ar^+ gas cluster ion while measuring the XPS. Although the etching depth of PP film cannot be directly calculated from the etching time, the hardness of the PP

material is similar to that of PLGA [poly (lactic-co-glycolic acid)], therefore the etching depth of the PP films can be derived from the calculation of PLGA.

Table 1-1. Chemical composition ratio before and after etching of PP film oxidized in 10 min at 25 and 90 °C.

Samples	Oxidized at 25 °C		Oxidized at 90 °C	
	C-O (%)	COO (%)	C-O (%)	COO (%)
Before etching	19.3	4.9	20.7	6.9
After etching (105 nm)	3.0	0.1	12.1	3.0
After etching (210 nm)	2.4	0.0	9.9	2.0

Table 1-1 shows the chemical composition of PP films oxidized at 25 and 90 °C for 10 min. In the case of 25 °C, the amount of oxygen decreased with increasing depth and the oxidized depth limit was determined to be about 110 nm. However, oxygen containing groups still existed on the surface of PP films treated at 90 °C after etching to depth of 210 nm (**Table 1-1** and **Figure 1-5**). These results clearly support that higher reaction temperature results in deeper oxidation depths. At nanometer range, the difference in the oxidation depth has a great influence on the adhesive strength. Furthermore, light activated $ClO_2^{\bullet}$ oxidation method can control the amount of incorporated oxygen at the thickness of nanometer level, and it can give strong adhesive ability without worsening the bulk physical properties of PP.

Electroless metal plating to oxidized PP

Both untreated and oxidized PP films were deposited into a sensitizer/activator solution and then immersed in a Cu plating solution (**Figure 1-6**a). After immersing for 1 min, both untreated and oxidized PP films were completely plated with Cu. After plating with Cu, the Cu layer of untreated PP film was completely removed after a tape test (**Figure 1-6**b left). On the contrary, good adhesion of Cu layer with the oxidized PP film was observed (**Figure 1-6**b right). Electroless Cu plating of PE and PVC films also gave similar results as shown in **Figure 1-6**c and d. Next, electroless Ni plating on PP, PE, and PVC was also studied by the same

methodology. As shown in **Figure 1-7**, all of the oxidized samples showed good adhesion with metal layer. The improvement in the adhesion of PP film surface with metal layer resulted from the interaction between the loaded catalyst of Pd^{2+} and the incorporated polar functional groups. These results indicate that the light-activated $ClO_2^{\bullet}$ oxidation method can be applied to the pre-treatment of metal plating for many polymers with similar chemical structure.

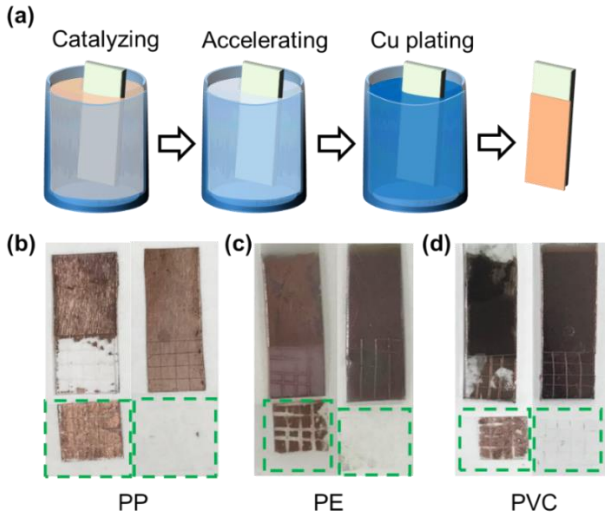

Figure 1-6. (a) Schematic diagram of the surface pretreatment for Cu plating. Pictures of Cu electroless plated (b) PP films, (c) PE plates, and (d) PVC plates after Scotch-tape test. Left and right are before and after oxidation, respectively.

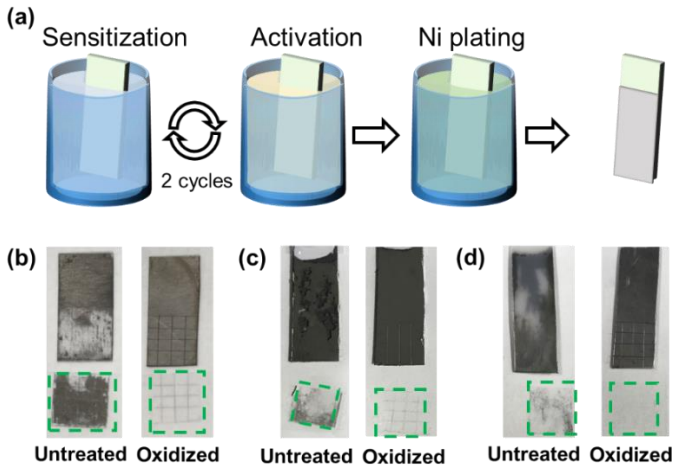

Figure 1-7. (a) Schematic diagram of the surface pretreatment for Ni plating; Pictures of electroless Ni plated (b) PP films; (c) PE plates and (d) PVC plates after Scotch-tape test.

Light activated $ClO_2^{\bullet}$ oxidation for porous three-dimensional substrate

In general, it is known that light irradiation on plastics can cause polymer chain scission. Thus, we studied several control experiments to investigate the effect of light irradiation on plastic surface and the active species in this surface oxidation. Here, in order to test the effect of UV irradiation on PP surface, the apparatus was set up (**Figure 1-8**b) to protect the PP film from UV while $ClO_2^{\bullet}$ was still generated.

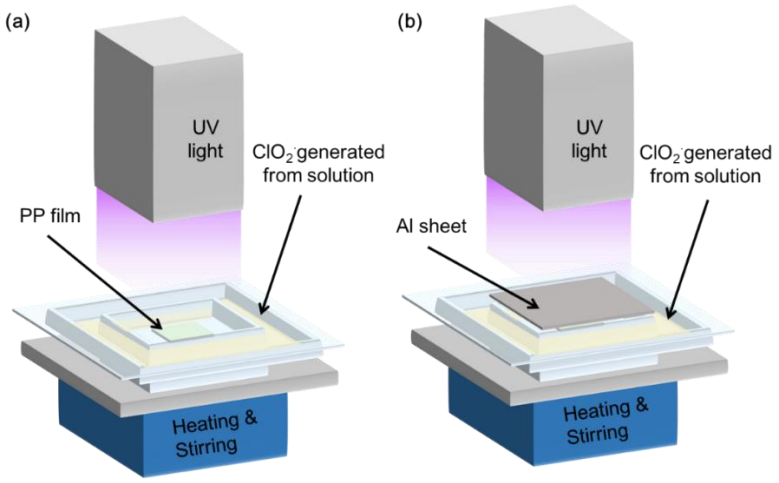

Figure 1-8. The schema of experimental method of oxidation of PP surface (a) UV irradiation for both $ClO_2^{\bullet}$ gas and polymer surface; (b) UV irradiation for only $ClO_2^{\bullet}$ gas.

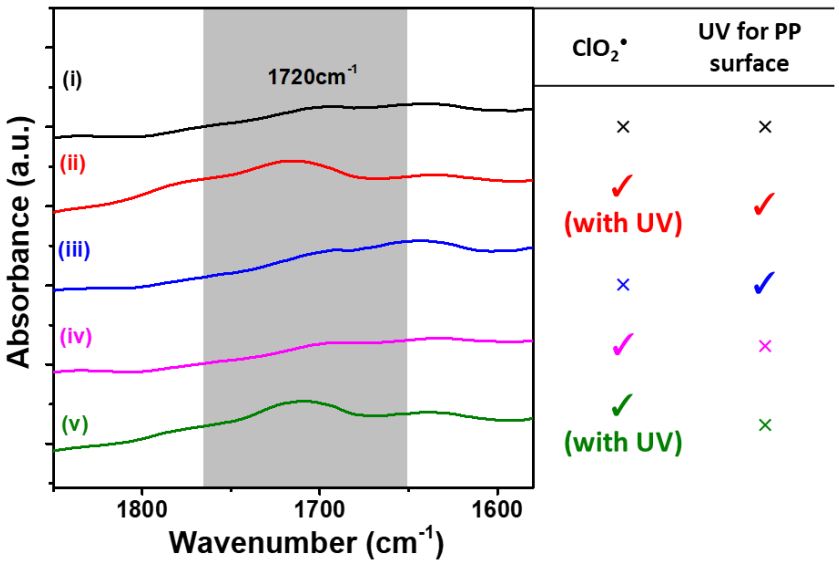

Figure 1-9. ATR-IR spectra of PP surface (i) untreated, (ii) treated under the UV irradiation with $ClO_2^{\bullet}$, (iii) treated under the UV irradiation without $ClO_2^{\bullet}$, (iv) treated under the dark with $ClO_2^{\bullet}$, (v) treated with light-activated $ClO_2^{\bullet}$ (no UV irradiation for PP surface during reaction) at 25 °C for 10 minutes.

According to the results of control experiments, it is found that UV irradiation is only required for the activation of chlorine dioxide radicals. That is to say, surface modification of polymers did not proceed by the direct light irradiation on PP surface using LED (365 nm) as light source. As shown in **Figure 1-9**, ATR-IR was employed to identify the incorporated functional groups. The spectrum (**Figure 1-9**-(i) and -(ii)) indicated the occurrence of surface oxidation: the reacted PP film showed new absorption peak at 1720 cm^{-1}, which corresponds to the introduction of carbonyl groups (C=O). These data revealed that the carboxyl groups were incorporated onto the PP film surface. Furthermore, it was found that the oxidation reaction did not proceed in the case of two control experiments, namely, the reaction was conducted under the UV irradiation on PP surface but in the absence of $ClO_2^{\bullet}$ gas (**Figure 1-9**-(iii)) and under the dark but in the presence of $ClO_2^{\bullet}$ gas (**Figure 1-9**-(iv)). On the other hand, PP was successfully oxidized under light activated (UV irradiated) $ClO_2^{\bullet}$ gas atmosphere without irradiation on PP surface. Additionally, the adhesion strength test of aluminum plate with the modified PP film that was oxidized at 90 °C for 10 minutes under light activated $ClO_2^{\bullet}$ gas atmosphere without irradiation on PP surface showed almost the same result (21±3.8 N/mm^2) with the result mentioned above (**Figure 1-4**c; 23±2.7 N/mm^2). Based on these results, we concluded that this novel oxidation was proceeded by the light-activated $ClO_2^{\bullet}$ radicals as active oxidant. Therefore, this novel modification method can be potentially used for complex plastics shapes where light cannot reach directly.

Then, we tried electroless plating of the mesh type PP, which has an internal void and a more complicated shape. As mentioned above, this novel surface oxidation was accomplished by light-activated $ClO_2^{\bullet}$ gas. Based on this fact, we considered that the gas could oxidize the internal void, and metal plating for a complicated structure would be possible. As expected, mesh type PP could also be successfully plated with copper (**Figure 1-10**a). The conductivity test of Cu plated PP film and PP mesh film by LED were conducted (**Figure 1-10**b). These results show that the light activated $ClO_2^{\bullet}$ oxidation method can be applied to pre-treatments of both metal-polymer adhesion and metal plating on polymers.

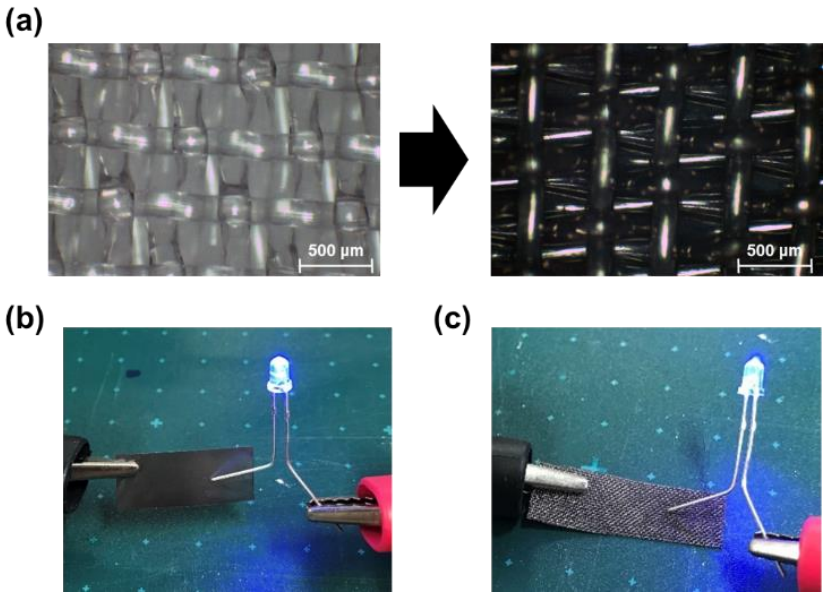

Figure 1-10. (a) Pictures of before and after Cu electroless plating on oxidized PP mesh film; (b) Pictures of conductivity test of Cu plated PP film (b) and PP mesh film (c) by LED.

1.4 Conclusions

This chapter demonstrated that PP film surface can be modified *via* the oxidation method using light-activated $ClO_2^{\bullet}$ and the adhesion of PP film with Al plate can be achieved after oxidation without any adhesives, as well the electroless metal plating on PP was achieved. We confirmed that the carbonyl groups were introduced onto film surface by IR and XPS measurements. Oxidation degree increased with increasing reaction time and temperature. It was found that the incorporation of polar groups in the depth direction increased as the reaction temperature was raised. The results show a positive correlation between the oxidation degree of PP and the adhesive strength. PP and metal could be firmly bonded by simple oxidation treatment on polymer surface. Because polar groups are easily introduced onto the surface of polymeric materials, the clean and energy-saving light activated $ClO_2^{\bullet}$ oxidation method is used as a novel platform for surface treatment of polymer substrates. In addition, it should be noted that the surface oxidation is caused by light-activated $ClO_2^{\bullet}$ gas indicating that this novel method is applicable to complex shape samples.

1.5 References

1. W. Brostow and H. E. Hagg Lobland, Materials: Introduction and Applications, John Wiley & Sons: West Sussex, UK, 2017, pp. 400–403.
2. R. Morent, N. De Geyter, C. Leys, L. Gengembre and E. Payen, *Surf. Interface Anal.*, 2008, **40**, 597–600.
3. C. Zhang, Y. Bai and W. Liu, *J. Adhes. Sci. Technol.*, 2014, **28**, 454–465.
4. M.R. Chashmejahanbin, A. Salimi and A. Ershad Langroudi, *Int. J. Adhes. Adhes.*, 2014, **49**, 44–50.
5. V. K. Thakur, D. Vennerberg and M. R. Kessler, *ACS Appl. Mater. Interfaces*, 2014, **6**, 9349–9356.
6. M. Jaritz, H. Behm, C. Hopmann, D. Kirchheim, F. Mitschker, P. Awakowicz and R. Dahlmann, *J. Phys. D. Appl. Phys.*, 2017, **50**, 015201.
7. J. Hrbacek, R. H. Pahler, W. Brostow, A. Hull, I. K. Chen, A. Srinivasan and N. Hnatchuk, *Polym. Test.*, 2017, **63**, 158–162.
8. F. Awaja, M. Gilbert, G. Kelly, B. Fox and P. J. Pigram, *Prog. Polym. Sci.*, 2009, **34**, 948–968.
9. S. J. Park and J. S. Jin, *J. Colloid Interface Sci.*, 2001, **236**, 155–160.
10. I. Novák and Š. Florián, *Macromol. Mater. Eng.*, 2004, **289**, 269–274.
11. M. Strobel and C. S. Lyons, *J. Adhesion Sci. Technol.*, 2003, **17**, 15–23.
12. M. Charbonnier, M. Romand, E. Harry and M. Alami, *J. Appl. Electrochem.*, 2001, **31**, 57–63.
13. M. Šimor, J, Ráhel', M. Černák, Y. Imahori, M. Štefečka and M. Kando, *Surf. Coatings Technol.*, 2003, **172**, 1–6.
14. S. Kreitz, C. Penache, M. Thomas and C. P. Klages, *Surf. Coatings Technol.*, **2005**, *200*, 676–679.
15. M. Charbonnier, *J. Electrochem. Soc.*, 1996, **143**, 472–480.
16. K. U. Inoue, K. Matsui, M. Watanabe and H. Honma, *Trans. IMF*, 2009, **87**, 51–54.
17. T. Tamai, M. Watanabe, Y. Kobayashi, Y. Nakahara and S. Yajima, *RSC Adv.*, 2017, **7**, 33155–33161.

18. D.-H. Kang, J.-C. Choi, J.-M. Choi, T.-W. Kim, *Trans. Electr. Electron. Mater.*, 2010, **11**, 174–177.
19. A. Garcia, T. Berthelot, P. Viel, A. Mesnage, P. Jégou, F. Nekelson, S. Roussel and S. Palacin, *ACS Appl. Mater. Interfaces*, 2010, **2**, 1177–1183.
20. N. Takeyasu, T. Tanaka, S. Kawata, *Japanese J. Appl. Physics, Part 2 Lett.*, 2005, **44**, L1134–L1137.
21. K. Ohkubo, H. Asahara and T. Inoue, *Chem. Commun.*, 2019, **55**, 4723–4726.
22. M. A. Chen, H. Z. Li and X. M. Zhang, *Int. J. Adhes. Adhes.*, 2007, **27**, 175–187.
23. M. R. Alexander, G. Beamson, C. J. Blomfield, G. Leggett and T. M. Duc, *J. Elect. Spect. Rel. Phenom.*, 2001, **121**, 19–32.

Chapter 2

Photooxidation of the ABS resin surface for electroless metal plating

2.1 Introduction

As mentioned in the general introduction, in recent years, metallization of plastics has attracted significant attention. The materials resulting from the combination of metals and plastics always have both the high mechanical strength and lightness of plastics with the reflectivity, electrical conductivity, and decorative properties of metals. Among plastic materials, ABS resin is one of the most widely applied thermoplastics owing to its inherent merits such as excellent toughness, processability, corrosion resistance, and low cost.[1-4] Electroless metal plating is one of the most useful metallizations because it is non-galvanic method without using any expensive equipment and a uniform surface can be obtained. Furthermore, electroless metal plating provides an electrically conductive substrate for further coating by electroplating and interactions between the plastic substrate and the metal layer.[5,6]

Before electroplating, plastic surfaces must be pretreated. Significant effort has been made toward investigating both physical and chemical modification methods. Among the studied modification methods, the application of a solution of chromic acid and sulfuric acid on the ABS resin surface has been used as the most popular treatment for the surface etching modification of the ABS resin surface for electroless plating.[7,8]. However, the use of chromic acid is limited because it is harmful to the environment. The high surface roughness resulting from the dissolution of PB improved the affinity of the metal to the ABS resin, but led to the loss of material. The ABS resin surface can also be successfully modified by the MnO_2-H_2SO_4 and MnO_2-H_2SO_4-H_3PO_4 etching systems; however, the problems of MnO_2 solubility and retention of MnO_2 on the ABS resin surface have limited their application.[9,10] Other chemical methods have also been investigated for surface modification such as photocatalytic reaction[11] and the use of ozonated water[12] and a mixture of acid with hydrogen peroxide[13]; however, they are not ideal methods for the adhesion of ABS resin to metal layer because of the weak adhesion

strength. Physical treatment of plasma[14,15] and optophysic treatment[16] have been proven to be effective for ABS resin surface modification; however, they can cause material loss and require high energy.

In chapter 1, surface oxidation of PP film, adhesive-free adhesion between an aluminum plate and surface-oxidized PP and successful electroless metal plating on surface-oxidized PP were achieved.[17] These results indicated that $ClO_2^{\bullet}$ oxidation can be applied as a surface modification method for plastics, and surface oxidation can result in the enhancement of adhesion between the metal layer and surface-oxidized plastics.

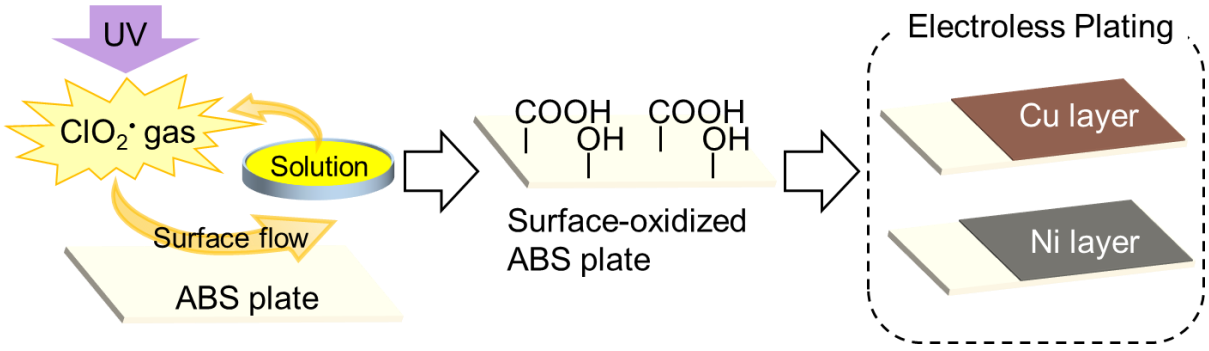

Figure 2-1. ABS resin plate surface modification *via* oxidation using light-activated $ClO_2^{\bullet}$ and following electroless plating.

Therefore, considering the serious problems caused by the previous environmentally harmful and inefficient methods, we applied the light-activated $ClO_2^{\bullet}$ for the oxidation of the ABS resin surface to develop a new modification method for pretreatment before electroless metal plating (**Figure 2-1**). Herein, the surface chemical composition, hydrophilicity, surface morphology, and adhesion of the metal layer after electroless plating were compared with those after the popular physical plasma treatment. Moreover, the effects of different oxidation reaction time and temperatures were investigated to obtain optimal conditions for electroless metal plating. Additionally, the oxidation of the ABS resin surface without direct UV irradiation on resin surface was studied, and an attempt was made to plate ABS resin with complex shapes printed by a 3D printer by copper.

2.2 Experimental section

Materials

Sodium chlorite ($NaClO_2$) was commercially obtained from Sigma-Aldrich (Tokyo, Japan). Hydrochloric acid was purchased from FUJIFILM Wako Pure Chemical Corporation (Osaka, Japan). Cu plating solutions (OPC-50 inducer M, OPC-150 Crystal RW, and ATS Addcopper IW) were kindly provided by Okuno Chemical Industry (Osaka, Japan). Ni plating reagents ($SnCl_2$, $PdCl_2$, $Ni_2SO_4 \cdot 6H_2O$, glycine, and $NaH_2PO_2 \cdot H_2O$) were purchased from Nacalai Tesque (Kyoto, Japan). Commercial ABS resin plates were purchased from AS ONE Corporation (Osaka, Japan).

Modification of the ABS resin plate surface

The ABS resin plate was oxidized by the $ClO_2^{\bullet}$ gas generated from an aqueous solution in a newly devised glassware described in the chapter 1. All samples were washed with water and dried in a vacuum drying oven before oxidation. For comparison, plasma treatment was conducted by treating the ABS resin plate for 10 s using a vacuum plasma equipment (Sakigake-Semiconductor, YHS-R).

Surface characterization

The static water contact angle was determined using Drop Master DM300 (Kyowa Interface Science, Saitama, Japan). In this study, 1.0 μL water droplet was fixed on the surface, and the contact angle was determined 5 s (scanning time) after the attachment of the droplet. The functional groups were determined by ATR-FTIR using the Nicolet iS5 spectrometer (Thermo Scientific, MA, USA) equipped with iD5 ATR accessory at room temperature. Elemental compositions of the surface were calculated using X-ray photoelectron spectroscopy (XPS; JEOL JPS-9010MC, Tokyo, Japan). The XPS parameters included the power of analysis (low resolution: 75 W, high resolution: 150 W) and monochromatic Al Kα. The survey and high-resolution XPS spectra were obtained at the fixed analyzer pass energies of 160 eV and 10 eV, respectively. Peak-differentiation-imitating analysis was performed by the CasaXPS Version 2.3.15 computer program. Data are presented as the mean ± standard deviation of five

independent experiments. The SU3500 scanning electron microscope (SEM; Hitachi, Tokyo, Japan), operated at 15 kV, was used for the observation of the morphological changes of the ABS resin plate surface. Before measurements, the ABS resin plates were adhered to the probe followed by coating with a thin layer of Au–Pd using an ion sputtering apparatus (E-1010 Hitachi Ltd., Tokyo, Japan). Oxidation of the ABS resin plate was determined by proton nuclear magnetic resonance (^{1}H-NMR) spectroscopy using JNM-ECS400 (400MHz, JEOL Ltd., Tokyo, Japan) and $CHCl_3$-d as a solvent.

2.3 Results and discussion

Surface analysis of modified ABS resin

Figure 2-2a shows the ATR-FTIR spectra of the ABS resin plate surface before and after treating with the light activated chlorine dioxide radical ($ClO_2^{\bullet}$). In the case of untreated ABS resin plate, the main absorption peaks around 2919 cm^{-1}, 2237 cm^{-1} and 1637 cm^{-1} assigned to C-H stretching vibration, C≡N stretching vibration and C=C stretching vibration, respectively. Compared with the untreated ABS resin plate, ABS resin plate surface-oxidized at 25°C in 10 min (encoded as **oxABS-25/10**) shows the absorption peak at 2919 cm^{-1} is obviously weakened, while a small new peak at 1710 cm^{-1} assigned to C=O appeared, which demonstrated that the oxygen containing group was incorporated onto the ABS resin plate surface and the light activated chlorine dioxide radicals could oxidize the C-H bond. The hydrophilicity of the ABS resin plate surface before and after oxidation was measured by water contact angle (**Figure 2-2**b). The results show the contact angle of **oxABS-25/10** (69.1±1.4°) was lower than that of the untreated samples (89.3±1.1°). The hydrophilicity of the ABS resin plate surface was improved after oxidation reaction.

ATR-FTIR (**Figure 2-4**a) and the water contact angle measurements (**Figure 2-4**b) were also conducted on the ABS resin plate before and after treatment with atmospheric plasma. The results show that the new absorption peak of C=O in the IR spectra obtained after oxidation

did not appear after the plasma treatment, but the peak intensity of C-H sharply decreased. The hydrophilicity of the ABS resin plate was improved after plasma treatment.

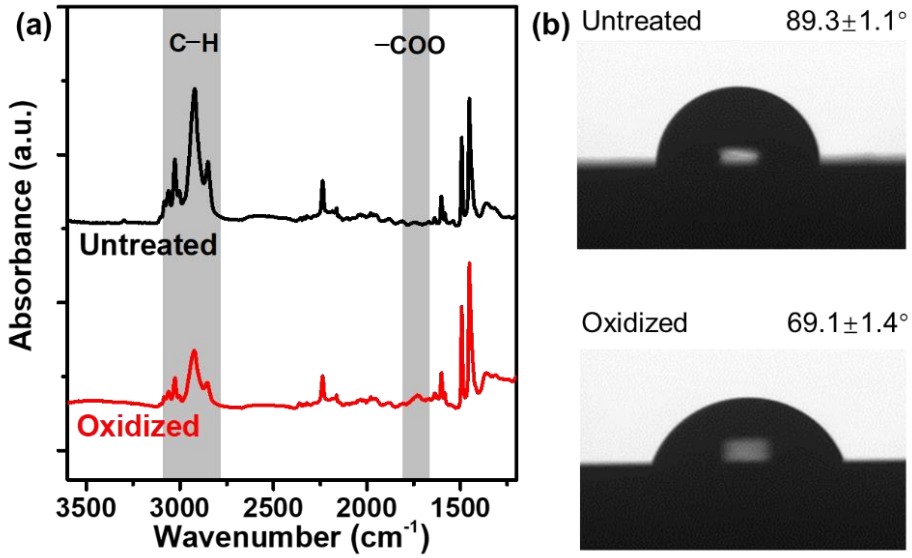

Figure 2-2. (a) ATR-FTIR spectra and (b) the water contact angles of the untreated ABS resin plate and **oxABS-25/10**.

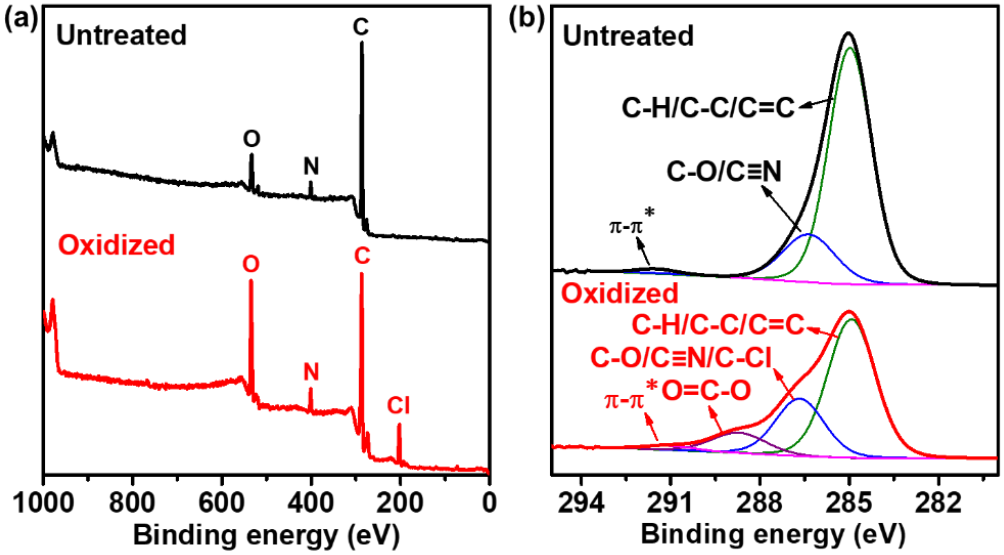

Figure 2-3. (a) Low-resolution XPS spectra and (b) C 1s high-resolution spectra of the untreated ABS resin plate surface and **oxABS-25/10** surface.

To comprehensively investigate the effect of oxidation on the chemical state of the ABS resin plate surface, the chemical composition and functional groups were determined by XPS

measurement. The polar groups introduced into the ABS resin plate surface oxidized with $ClO_2^{\bullet}$ were also determined from the curve fitting of the C 1s high-resolution spectra. **Figure 2-3**a shows the low-resolution XPS spectra of the untreated ABS resin plate and **oxABS-25/10**, and the C 1s high-resolution spectra are displayed in **Figure 2-3**b. In the low-resolution XPS spectra of the untreated ABS resin plate, a main peak around 285 eV corresponding to carbon and a peak around 400 eV corresponding to nitrogen are observed. Oxygen also existed in the untreated ABS resin plate because of the inevitable incorporation of oxygen from the industrial production process. After oxidation, the amount of oxygen on the ABS resin plate surface significantly increased (from 7.84% to 17.22%) and a small amount of chlorine was introduced into the ABS resin plate surface. The C 1s high-resolution spectrum of the untreated ABS resin plate indicated three peaks due to C–C, C–H, and C=C (284.9 eV), C–O and C≡N (286.4 eV), and π–π* (291.9 eV). After oxidation for 10 min at 25°C, new peaks appeared due to the incorporation of the -COO groups (289.0 eV) and C-O/C-Cl (286.5 eV). Although the peak at 286.5 eV is difficult to be deconvoluted into the peaks of the C–O, C–Cl, and C≡N groups, the results reveal that the amount of the C-O/C-Cl groups increased after oxidation. The incorporation of polar functional groups *via* oxidation is beneficial to the adhesion of the polymer to metal. Herein, the introduction of trace amounts of C–Cl groups is also an unignorable reason for the adhesion between the metal layer and polymer. In contrast, less oxygen (**Figure 2-4**c) and oxygen-containing groups (**Figure 2-4**d) were incorporated into the plasma-treated ABS resin plate surface, and these polar functional groups evolved their orientation and migration into the bulk polymer.[18,19]

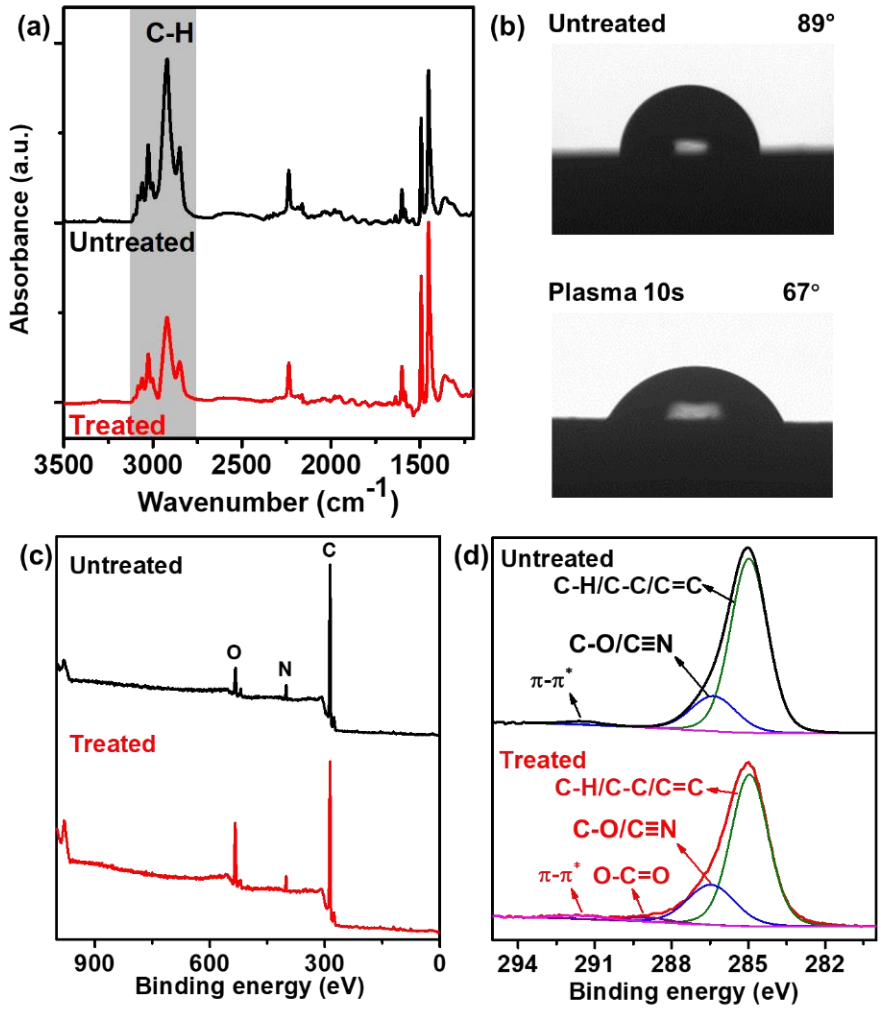

Figure 2-4. (a) ATR-FTIR spectra of the untreated ABS resin plate and ABS resin plate treated with plasma for 10 s; (b) the water contact angles of the ABS resin plate before and after treatment; and (c) XPS wide scan spectra and (d) C1s spectra of the untreated ABS resin plate surface and plasma-treated ABS resin plate surface (10 s).

The time stability of the ABS resin oxidized by this method in our study was investigated. After 4 months, the amounts of oxygen and polar functional groups on the surface were determined by XPS. Only a slight decrease was observed in the oxygen amount (from 16.14% to 15.67%) and polar functional groups (taking carboxylic groups as an example: from 8.78% to 8.07%). This result revealed that herein, oxidation retarded the rotation and migration of polar functional groups. Moreover, the surface asperities induced by plasma treatment cause surface deterioration.

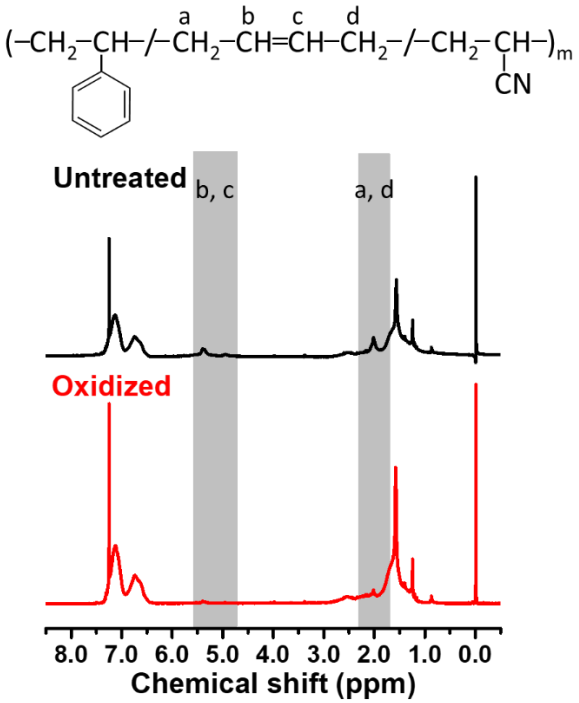

Figure 2-5. ^{1}H-NMR spectra of the untreated ABS resin plate surface and **oxABS-25/10** surface (five pieces of the oxidized ABS resin plate surface were rinsed with $CHCl_3$, and $CHCl_3$ was evaporated. The remnant was dissolved in $CDCl_3$).

As ABS resin is a kind of copolymer of three monomers of acrylonitrile, butadiene, and styrene, ^{1}H-NMR spectroscopy was conducted to confirm the oxidized part of the ABS polymer chain. In the ^{1}H-NMR spectra (**Figure 2-5**) of the ABS resin plate surface before and after oxidation, the chemical shift of 5.3 ppm, corresponding to the protons of -HC=CH- in butadiene, decreased after oxidation. Moreover, the chemical shift of 2.0 ppm, corresponding to the proton of $-CH_2-$ located beside -HC=CH-, decreased after oxidation. Both results indicated that the -HC=CH- bond of butadiene in ABS resin was broken by $ClO_2^{\bullet}$ during oxidation and PB was the oxidized part.

It is important to observe the microscopic appearance of the untreated ABS resin plate and **oxABS-25/10** to examine the morphological changes of the ABS resin plate surface after oxidation. The purchased ABS resin plate surfaces are smooth and hydrophobic due to the lack of polar functional groups on them (**Figure 2-6**a), which cannot provide a mechanical or chemical anchorage to the metallic deposit. The **oxABS-25/10** surface is rough with nano-

bubbles/holes (**Figure 2-6**b). For comparison, the morphology of the plasma-treated ABS resin plate surface was observed by SEM (**Figure 2-6**c). A large number of smaller bubbles/holes were created by the plasma treatment, which led to a rougher ABS resin plate surface.

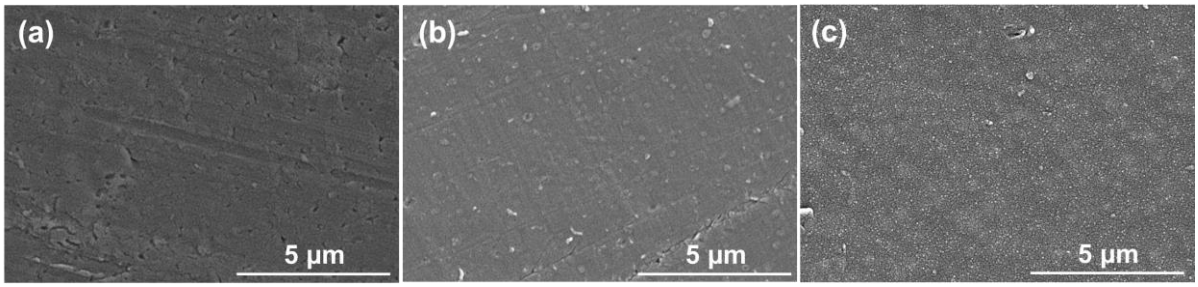

Figure 2-6. SEM images of the (a) untreated ABS resin plate surface, (b) ABS resin plate surface oxidized at 25 °C for 10 min, and (c) ABS resin plate surface treated by plasma for 10 s.

Effects of oxidation conditions

The effects of oxidation time on the chemical component ratio, surface hydrophilicity, and surface morphology were investigated to reveal the relationship between the oxidation conditions and oxidation degree. The ABS resin plates were oxidized for different durations of oxidation at room temperature. **Figure 2-7**a and c show the surface chemical component ratio after oxidation for different durations. Although before and after oxidation, a significant increase in the oxygen amount and polar functional group ratio was observed on the ABS resin plate surface, the rate of increase sharply decreased with the increasing oxidation time. When the oxidation time was increased to 30 min, the oxygen amount and polar functional group ratio no longer increased. Specifically, oxidation occurs rapidly and is finished in a short time, which is beneficial for industrial use. Moreover, the water contact angles (**Table 2-1**) of the ABS resin plates oxidized for different durations of oxidation were almost the same, which is in accordance with the XPS results. SEM images (**Figure 2-8**) display the difference between the surface morphologies of the ABS resin plates oxidized for different durations of oxidation, and the results reveal that the number of nano-bubbles/holes on the surface and roughness increased with the increasing oxidation time. Longer oxidation time resulted in more surface damage. To

obtain a comparably high oxidation degree in a shorter time while avoiding surface damage, the optimal oxidation time was determined to be 10 min. This oxidation is considered to be a "self-limiting" process, meaning that the oxidation produces a surface that prevents further oxidation.

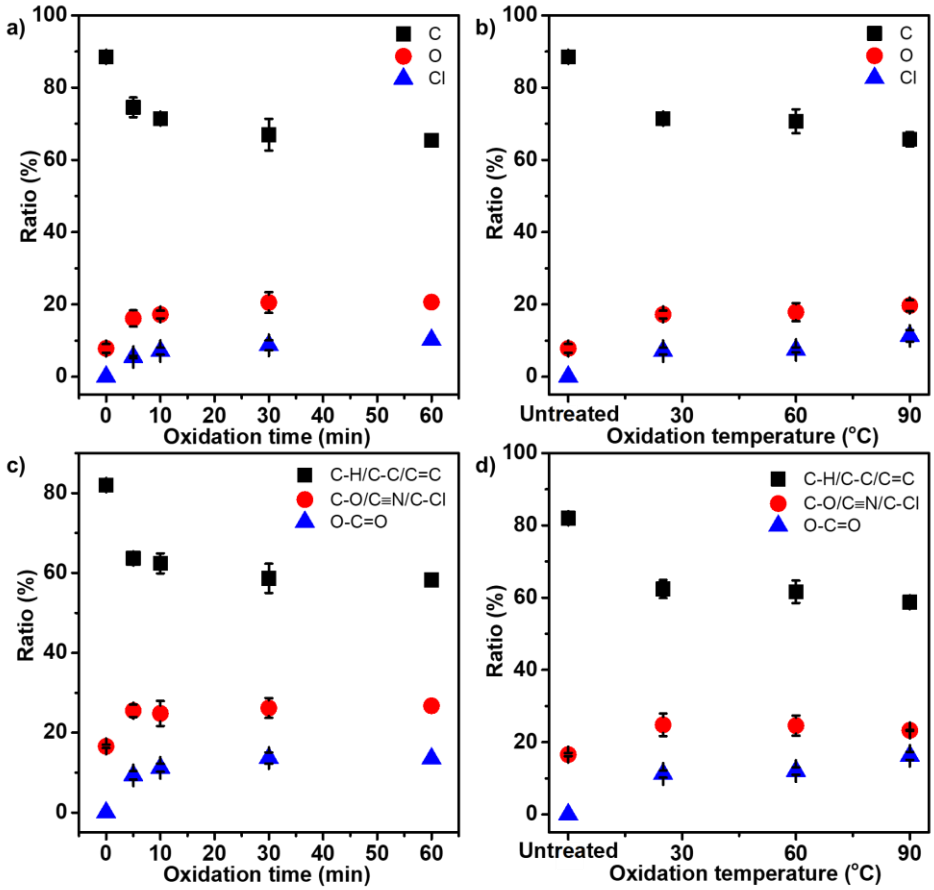

Figure 2-7. Relation of oxidation time with chemical component ratio calculated from the low-resolution spectra (a) and C 1s high-resolution spectra (c). Relation of oxidation temperature with chemical component ratio calculated from the low-resolution spectra (b) and C 1s high-resolution spectra (d). Data are displayed as mean ± standard deviation of three independent experiments.

Table 2-1. Water contact angles (WCAs) of the ABS resin plate surface oxidized under different conditions.

Oxidation condition	untreated	25 °C				60°C	90°C
		5 min	10 min	30 min	60 min	10 min	10 min
WCAs	89±1.1	69±1.4	69±2.9	69±2.8	67±3.1	68±4.1	62±0.5

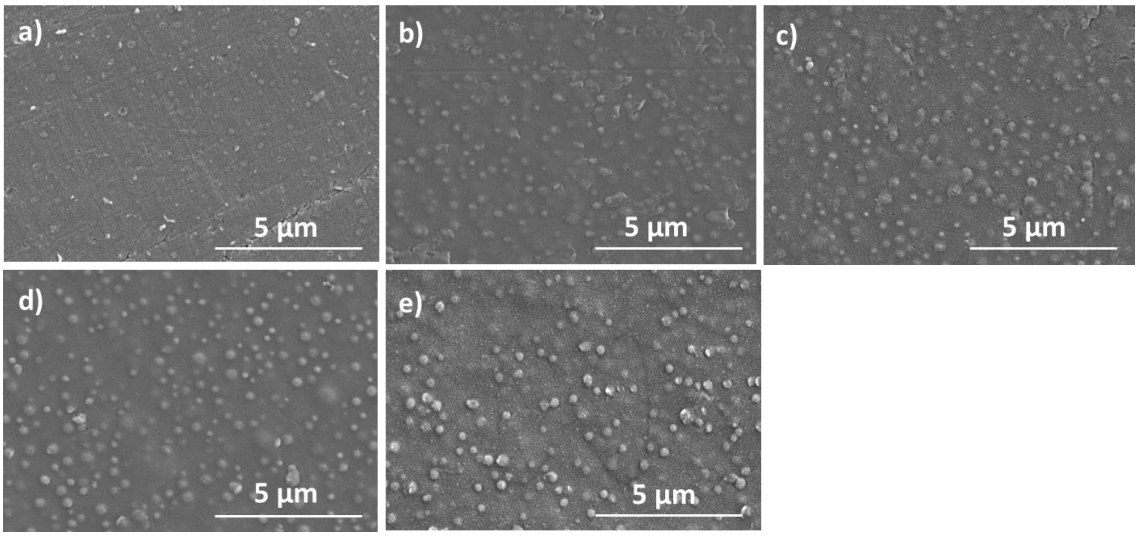

Figure 2-8. SEM images of the ABS resin plate surface oxidized at (a) 25 °C for 10 min, (b) 25 °C for 30 min, (c) 25 °C for 60 min, (d) 60 °C for 10 min, and (e) 90 °C for 10 min.

The effect of the oxidation temperature was also investigated. **Figure 2-7**b and d display the surface chemical component ratios after oxidation for 10 min at different temperatures. After oxidation at 25 °C for 10 min, the oxygen ratio reached 17.22% and the carboxylic group ratio reached 11.21%. With an increase in the oxidation temperature, the oxygen ratio and carboxylic group ratio slightly increased and the ratio of the other polar groups no longer increased. The SEM images (**Figure 2-8**a, d and e) show that the number of nano-bubbles/holes on the surface and roughness increased with an increase in the oxidation temperature. To summarize, the optimal oxidation time and temperature were determined to be 10 min and 25 °C, respectively.

Electroless metal plating of modified ABS resin

After the polar functional groups were confirmed to be incorporated into the ABS resin plate surface by oxidation *via* $ClO_2^{\bullet}$, both the untreated ABS resin plate and **oxABS-25/10** were exposed to electroless plating using Cu and Ni described in the chapter 1. After electroless plating, the adhesion of the metal layer to the surface of the resin plates was tested by the Scotch tape test (**Figure 2-9**). According to the Cu electroless plating described in the Experimental section, the samples were placed in a sensitizer/activator solution and then immersed in a Cu

plating solution. Both the untreated ABS resin plate and **oxABS-25/10** were completely covered by a thin Cu layer after 1-minute immersion. However, after the Scotch tape test, the Cu layer on the untreated ABS resin plate was completely removed (**Figure 2-9**a), while strong adhesion of the Cu layer to **oxABS-25/10** was observed. Ni electroless plating was also conducted *via* the method shown in the Experimental section. After immersion in the Ni solution for 20 min, **oxABS-25/10** was fully plated, while the untreated ABS resin plate was rarely plated (**Figure 2-9**b). Moreover, the Ni layer on the plated **oxABS-25/10** was not removed by the tape test. The strong adhesion of the metal layer to the ABS resin plate was achieved by surface oxidation *via* $ClO_2^{\bullet}$, which can be used as a basic treatment for the next electro-metal plating. The improved adhesion between the modified ABS resin plate and the deposited metal layer is attributed to the chemical interaction between the incorporated polar functional groups as well as the slightly rough surface created herein, and the former is the main reason. For comparison, the plasma-treated ABS resin plate was plated with Cu (**Figure 2-9**c). The result indicated that the ABS resin plate treated by oxidation has a comparable adhesion property with the traditional physically plasma-treated ABS resin plate. However, the polar functional groups induced by plasma treatment suffer from the rotation and migration and plasma treatment cause more surface deterioration. The effects of oxidation conditions on electroless Cu plating were also investigated (**Figure 2-10** and **Table 2-2**). The ABS resin plates oxidized for different durations at room temperature were completely covered by a Cu layer, and all samples passed the Scotch tape test. The sample oxidized at 60°C was not completely covered by the Cu layer and part of the deposited Cu layer was removed after the tape test. The Cu layer deposited on the samples oxidized at 90 °C turned dark after electroless plating.

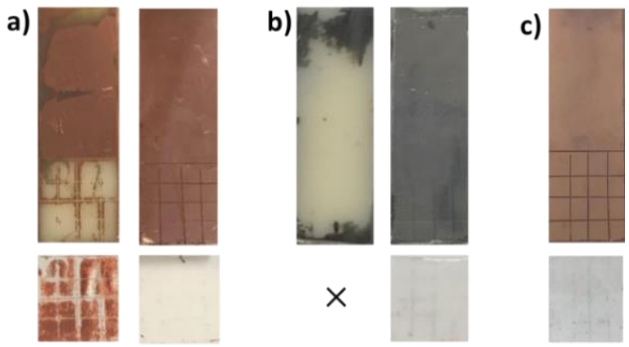

Figure 2-9. Images of the (a) Cu electroless-plated and (b) Ni electroless-plated ABS resin after the Scotch tape test. Left and right images were obtained before and after oxidation, respectively. (c) The Cu electroless-plated ABS resin treated by plasma for 10 s after the Scotch tape test.

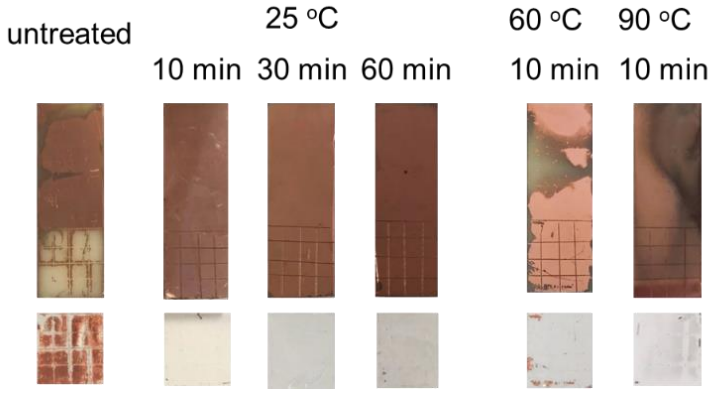

Figure 2-10. Images of the Cu electroless-plated ABS resin oxidized under different conditions.

Table 2-2. Scotch tape test results of the Cu electroless-plated ABS resin plates oxidized under different conditions.

Oxidation conditions	Untreated	25°C			60°C	90°C
		10 min	30 min	60 min	10 min	10 min
Removal Ratio	16/16	0	0	0	2/16	0

In a previous study on PP oxidation using this method, it was demonstrated that UV irradiation is only required for the activation of $ClO_2^{\bullet}$.[17] In this study, we investigated the oxidation process *via* UV-activated $ClO_2^{\bullet}$ on the ABS resin plate surface without UV

irradiation on the ABS resin plate surface. The water contact angle and XPS measurements were conducted to observe the hydrophilicity and oxidation degree (**Table 2-3**). The results revealed that the hydrophilicity of the ABS resin plate surface was improved and oxygen-containing groups were incorporated into the ABS resin plate surface after oxidation *via* UV-activated $ClO_2^{\bullet}$ without UV irradiation on the ABS resin surface. Under the same conditions of oxidation time and temperature (10 min and 25 °C, respectively), the ratio of oxygen and polar groups on the ABS resin plate surface oxidized without UV irradiation on the surface was significantly lower than that for **oxABS-25/10**; however, with the increasing oxidation time or temperature, the oxidation degree reached the same level. These results indicate that the rate of oxidation was lower without UV irradiation on the ABS resin surface. Moreover, electroless plating was conducted on the ABS resin, which had an internal void and a more complicated shape (**Figure 2-11**). Because the $ClO_2^{\bullet}$ gas was applied as an oxidant to modify the ABS resin surface, it can reach even the back side of the ABS resin which cannot be exposed to the light. As expected, the ABS resin with a complicated shape could also be successfully plated with copper including internal surfaces. These results show that the light-activated $ClO_2^{\bullet}$ oxidation method can be applied as an effective pretreatment for the electroless plating of ABS resin.

Table 2-3. Water contact angles (WCAs) and chemical component ratios calculated from the XPS measurement of the ABS resin plates surface oxidized under different conditions without UV irradiation on the ABS resin surface.

Oxidation conditions (no UV on surface)	WCAs (°)	Atomic ratio (%)						
		C	O	N	Cl	C-H/C-C/C=C	C-O/C≡N/C-Cl	O-C=O
25°C@5 min	83	88.75	6.66	3.79	0.80	80.03	16.29	1.90
25°C@10 min	75	83.57	11.26	3.21	1.96	75.76	17.32	5.20
25°C@30 min	75	75.99	16.97	3.27	3.77	67.32	23.58	7.72
60°C@10 min	74	70.62	18.69	3.34	7.35	63.86	23.64	11.37
90°C@10 min	69	64.71	22.53	3.44	9.32	61.34	20.43	16.92

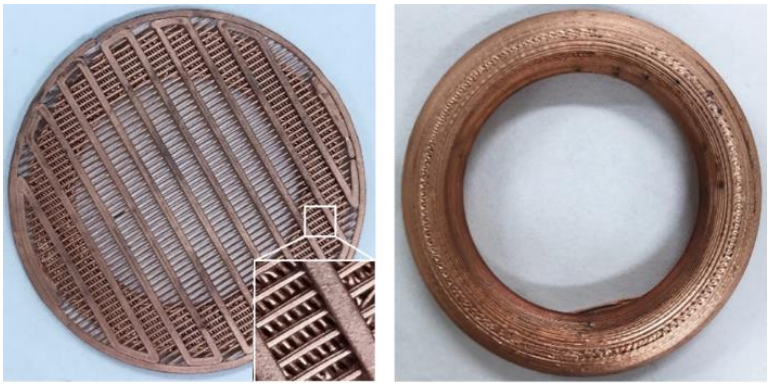

Figure 2-11. Images of Cu electroless-plated ABS resin with different complex structures printed by a 3D printer (image inside the left part shows partially magnified details).

2.4 Conclusions

In this chapter, oxidation *via* light-activated $ClO_2^{\bullet}$ was demonstrated to be useful for the modification of the ABS resin surface, which could be applied as an effective alternative pretreatment for the electroless plating of ABS resin instead of the traditional methods. Herein, the improvement of the ABS resin surface hydrophilicity was revealed by the water contact angle measurement, and the polar groups, including the carboxylic groups, were confirmed to be incorporated into the ABS resin surface by IR and XPS measurements. The oxidized portion of the ABS resin was proved to be PB by H-NMR spectroscopy. Electroless metal plating could be achieved after simple oxidation modification of the ABS resin plate surface. According to the oxidation degree and the electroless plating results, the optimal oxidation conditions were determined to be 10 min and 25 °C, and the reaction was fast under these mild conditions. It should also be noted that the surface oxidation of ABS resin did not require direct light-irradiation on the surface, which led to the successful plating of ABS resin with complex shapes. Compared with the commercial wet chemical process, this modification is an environmental-friendly process without causing significant surface damage, while identical electroless plating results were also obtained. Thus, this oxidation method is a clean and effective approach for the modification of ABS resin surface due to the ease of induction of polar groups and its energy efficiency.

2.5 References

1. H. N. Zhang, J. Wang, F. F. Sun, D. Liu, H. Y. Wang and F. Wang, *Bull. Mater. Sci.* 2014, **37**, 71–76.
2. Z. Shu and X. Wang, *Appl. Surf. Sci.*, 2012, **258**, 5328–5331.
3. S. Olivera, H. B. Muralidhara, K. Venkatesh, K. Gopalakrishna and C. S. Vivek, *J. Mater. Sci.*, 2016, **51**, 3657–3674.
4. A. Garcia, T. Berthelot, P. Viel, A. Mesnage, P. Jégou, F. Nekelson, S. Roussel and S. Palacin, *ACS Appl. Mater. Interfaces*, 2010, **2**, 1177–1183.
5. F. Basarir, *ACS Appl. Mater. Interfaces*, 2012, **4**, 1324–1329.
6. T. Tamai, M. Watanabe, Y. Kobayashi, Y. Nakahara and S. Yajima, *RSC Adv.*, 2017, **7**, 33155–33161.
7. W. Gui-xiang, L. Ning, H. Hui-li and Y. Yuan-chun, *Appl. Surf. Sci.*, 2006, **253**, 480–484.
8. A. P. Kurek, M. E. R. Dotto, P. H. H. de Araújo and N. Sellin, *J. Appl. Polym. Sci.*, 2017, **134**, 1–10.
9. Z. Yang, Y. He, Z. Li, N. Li and Z. Wang, *J. Adhes. Sci. Technol.*, 2011, **25**, 1211–1221.
10. W. Zhao, J. Ding and Z. Wang, *Langmuir*, 2013, **29**, 5968–5973.
11. W. Zhao, Q. Ma, L. Li, X. Li and Z. Wang, *J. Adhes. Sci. Technol*., 2014, **28**, 499–511.
12. T. Nomura, H. Nakagawa, K. Tashiro, Y. Umeda, H. Honma and O. Takai, *Trans. Inst. Met. Finish*., 2016, **94**, 322–327.
13. L. A. C. Teixeira and M. C. Santini, *J. Mater. Process. Technol*. 2005, **170**, 37–41.
14. J. Abenojar, R. Torregrosa-Coque, M. A. Martínez and J. M. Martín-Martínez, *Surf. Coatings Technol*., 2009, **203**, 2173–2180.
15. H. Song, J. M. Choi and T. W. Kim, *Trans. Electr. Electron. Mater.*, 2013, **14**, 133–138.
16. L. Magallón Cacho, J. J. Pérez Bueno, Y. Meas Vong, G. Stremsdoerfer, F. J. Espinoza Beltrán and J. Martínez Vega, *J. Coatings Technol. Res.*, 2015, **12**, 313–323.
17. Y. Jia, J. Chen, H. Asahara, T. Asoh and H. Uyama, *ACS Appl. Polym. Mater.*, 2019, **1**, 3452–3458.

18. J. Friedrich, I. Loeschcke, H. Frommelt, H. D. Reiner, H. Zimmermann and P. Lutgen, *Polym. Degrad. Stab*. 1991, **31**, 97–114.

19. W. J. Brennan, W. J. Feast, H. S. Munro, S. Walker, *Polymer*, 1991, **32**, 1527–1530.

Chapter 3

Surface modification of polycarbonate using the light-activated chlorine dioxide radical

3.1 Introduction

Polycarbonate (PC) is one of the most commonly used polymers owing to its specific properties, such as transparency, high mechanical strength, light weight, high electrical insulation, and high temperature resistance,[1-3] which make it a suitable alternative for conventional engineering materials. Biocompatible PC plastic, a type of bio-based degradable polymer, can be widely used for different purposes, including optical applications, food contact materials, medical devices, and digital optical data storage discs.[4-6] Furthermore, owing to its facile fabrication, PC plastic is widely commercially available. However, PC presents certain drawbacks, such as poor hydrophilicity and adhesion properties;[7,8] therefore, the surface of commercial PC plastic should be properly modified to expand its applications. To date, both physical and physical-chemical treatments, including plasma[9-12], laser[13,14], ion beam[15-17] and ultraviolet (UV)-ozone[18] treatments, have been studied for the modification of PC surface. However, all these treatments require high costs and hazardous operating conditions and cannot be used for complex geometric shapes. In addition, the polar functional groups induced via plasma treatment suffer from rotation and migration in the days following the treatment, and the transmittance of PC decrease after plasma treatment,[19,20] the use of ion beams on polymeric material induces irreversible changes in their macromolecular structure, and UV-ozone causes C–C bond cleavage, resulting in significant decrease in the molecular weight of the plastics.[21] Therefore, these treatments are not ideal for the surface modification of PC, and consequently, the demand for fast, efficient, energy-saving, and safe surface treatment processes has increased.

In this study, according to the modification *via* oxidation mentioned in the general introduction and used in the chapter 1 and 2, the modification of the PC film surface achieved

using light-activated $ClO_2^{\bullet}$ was confirmed using X-ray photoelectron spectroscopy (XPS) and proton nuclear magnetic resonance (^{1}H-NMR). The hydrophilicity and surface morphology of the PC film surface after oxidation were also analyzed. The oxidation conditions, viz. the oxidation time and temperature, were investigated to reveal their effects on the oxidation degree, chemical composition, and hydrophilicity of the PC film surface. Moreover, since transmittance is a key property for the applications of PC, the effect of oxidation temperature on PC plates transmittance is also studied. These results were used to determine the optimal reaction conditions. In addition, after PC films surfaces were oxidized using light-activated $ClO_2^{\bullet}$, they were subjected to electroless plating which is a useful metallization method.

3.2 Experimental section

Materials

Sodium chlorite ($NaClO_2$) and hydrochloric acid (HCl) were purchased from Sigma-Aldrich (Tokyo, Japan) and FUJIFILM Wako Pure Chemical Corporation (Osaka, Japan), respectively. Cu plating solutions (OPC-50 inducer M, OPC-150 Crystal RW, and ATS Addcopper IW) were kindly provided by Okuno Chemical Industry (Osaka, Japan). The Ni plating reagents (tin (II) chloride ($SnCl_2$), palladium (II) chloride ($PdCl_2$), nickel (II) sulfate hexahydrate ($NiSO_4 \cdot 6H_2O$), glycine, and sodium hypophosphite monohydrate ($NaH_2PO_2 \cdot H_2O$)) were purchased from Nacalai Tesque (Kyoto, Japan). PC films (with a glass transition temperature of 148 °C) were purchased from AGC Inc. (Tokyo, Japan) and PC plates with the same chemical structure as PC films were provided by NAGASE & CO., LTD (Osaka, Japan)

Oxidation of PC film/plate surface

The PC film/plate surface was oxidized using UV-activated $ClO_2^{\bullet}$ gas, which was generated *via* the irradiation on an aqueous solution described in the chapter 1. A watch glass system was set up to perform the oxidation of the PC film/plate surface using the procedure

described in the chapter 1. The commercial PC films and plates were cut into the area of $3\times1cm^2$ with the thickness of 0.18 mm and 0.5 mm, respectively. The PC films/plates were placed inside the watch glass system and the aqueous solution filled the outermost part of the glassware. Both the PC films/plates and aqueous solutions were irradiated using UV light. All the samples were washed with water and dried in a vacuum oven at 25 °C before oxidation. The oxidized samples were also washed with water and dried in a vacuum oven at 25 °C prior to tests. After modification, the used solution was irradiated by the UV light until the excess $ClO_2^{\bullet}$ was completely decomposed.

Characterization

The surface chemical composition of the PC films was determined using an JPS-9010MC XPS (JEOL, Tokyo, Japan) instrument. The XPS inert parameters included the power of analysis (wide: 75 W, narrow: 150 W) and monochromatic Al Kα radiation. The survey and high-resolution XPS profiles were obtained at the constant analyzer pass energies of 160 and 10 eV, respectively. The CasaXPS Version 2.3.15 software was used for the peak-differentiation-imitating analysis of the C1s narrow XPS profile. Three independent experiments were conducted to obtain the standard deviation of the data. The static water contact angles of the PC films were determined using a Drop Master DM300 (Kyowa Interface Science, Saitama, Japan) contact angle meter. A 1.0-μL water droplet was placed on the surface of the PC film, and the contact angle was determined 5 s (scanning time) after the attachment of the droplet. The functional group composition of the PC film surface was determined using ^{1}H-NMR spectroscopy utilizing a JNM-ECS400 (400 MHz, JEOL, Tokyo, Japan) instrument and deuterated dimethylformamide (DMF-d_7) as the solvent. A SU3500 scanning electron microscopy (SEM; Hitachi, Tokyo, Japan) device operated at 15 kV was used for the observation of the morphological changes of the PC films surface. Before measurements, the PC films surface was adhered to the probe and then it was coated with a thin Au–Pd layer using an E-1010 (Hitachi, Tokyo, Japan) ion sputtering apparatus. The transmittance of the PC plates was determined using a U-2810 (Hitachi, Tokyo, Japan) ultraviolet–visible (UV–vis)

spectrophotometer and a haze meter (NDH-4000, Nippon Denshoku, Tokyo, Japan) was employed to measure the haze values.

3.3 Results and Discussion

Surface modification of PC film via oxidation

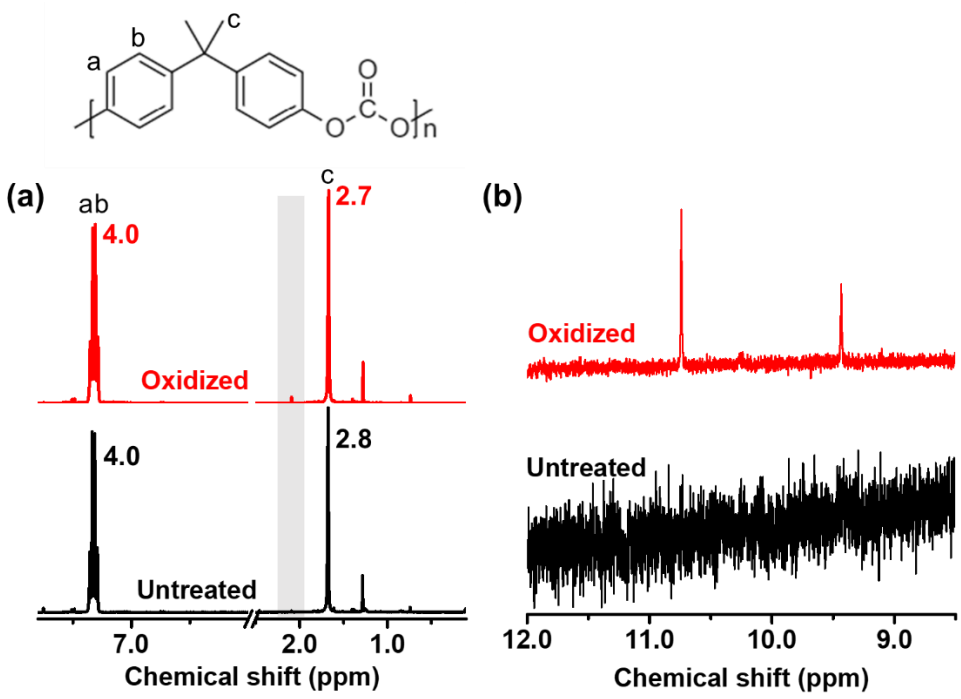

Figure 3-1. Proton nuclear magnetic resonance spectra of the untreated PC film and **oxidized PC** surface. Chemical shifts (δ) ranged from (a) 0.2 to 7.8 and (b) 8.5 to 12.0. Here, **oxidized PC** denotes PC film oxidized using light-activated $ClO_2^{\bullet}$ at 25 °C for 10 min.

The chemical structures of the untreated PC film surface and PC film surface oxidized using light-activated $ClO_2^{\bullet}$ at 25 °C for 10 min (hereafter **oxidized PC**) were confirmed using ^{1}H NMR. To prepare the surface of the **oxidized PC** samples, five **oxidized PC** samples were rinsed with DMF to dissolve their surface. Then, DMF was evaporated and the residual substance was dissolved in DMF-d_7 and was subsequently subjected to ^{1}H NMR analysis. **Figure 3-1** presents the ^{1}H-NMR spectra of the untreated PC film and **oxidized PC** surfaces. The peak of the aromatic protons in the range of 7.3-7.4 ppm and that of the methyl protons at

1.67 ppm, which were assigned to the main chain of PC, were observed in **Figure 3-1**a. After oxidation, the intensity of the peak of the methyl protons (1.67 ppm) slightly decreased and that of the peak of the hydroxyl proton of Ph–C–OH (2.09 ppm) increased. Furthermore, new peaks at the chemical shifts of 10.8 and 9.7 ppm, which were assigned to the carboxyl and aldehyde protons, respectively, appeared in the spectrum of **oxidized PC** (**Figure 3-1**b). The oxidation mechanism of PC was complicated and comprehensive. In this study, the mechanism was supposed as follows: According to the feasible reaction mechanism for the oxygenation of PP,[21] the activation and oxygenation of C-H on PC occurred selectively at the side-chain methyl groups rather than at the phenyl groups, which was supported by the absence of the Ph–OH (δ = 6.7) peak from the 1H-NMR spectra of **oxidized PC**. Another hypothesis is also proposed. After activation and dehydrogenation of the C-H in the methyl groups in the side chain, the subsequent isomerization provides an activated site in the quaternary carbon in the main chain of PC (**Figure 3-2**),[22] which is supported by the presence of the Ph-C-OH. Besides, the C-O bond cleavage in the -O-(C=O)-O- did not occurred due to the absence of the Ph-OH.

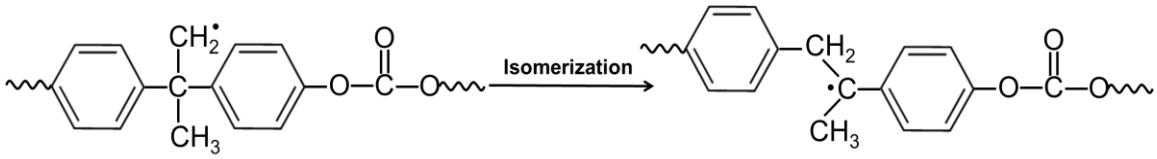

Figure 3-2. Scheme of the isomerization after activation and dehydrogenation of the C-H in the methyl groups.

In addition, XPS measurements were conducted to determine the surface chemical composition and identify the functional groups of the PC films. The survey and C1s narrow XPS profiles of the untreated PC film and **oxidized PC** surface are illustrated in **Figure 3-3**a and b, respectively. Two peaks at approximately 285 and 532 eV, which corresponded to C and O, respectively, were observed in the survey profiles of untreated PC film and **oxidized PC** surface. The ratio of O on the surface of untreated PC film was [18].71% and that of **oxidized PC** was increased to 22.15%; moreover, a small amount of Cl was detected on the surface of the **oxidized PC** sample (**Figure 3-3**a). The polar groups introduced on the surface of **oxidized**

PC were also identified using the curve fitting of the C1s narrow profile. The C1s narrow profile of untreated PC was deconvoluted into four peaks with the following binding energies and assignments: (1) 285 eV, aromatic and aliphatic carbon; (2) 286.5 eV, C–O; (3) 290.5 eV, –O–(C=O)–O–, and (4) 291.5 eV, π-π* transitions. After PC was oxidized for 10 min at 25 °C, a new peak at 289.0 eV appeared in its spectra, and that was ascribed to the introduction of the –COO groups on the surface of **oxidized PC**. Although it was difficult to distinguish the peaks ascribed to the C–O and C–Cl polar groups, the intensity of the peak at 286.5 eV, which corresponded to the C–O/C–Cl groups, was increased. In this study, the introduction of the small amount of C–Cl polar groups on the surface of **oxidized PC** was also considered to be an important reason for the improvement in the hydrophilicity and adhesion with heterogeneous materials of **oxidized PC**. These results indicated that this oxidation method using light-activated $ClO_2^{\bullet}$ was effective for the introduction of functional groups on the PC film surface. Furthermore, the XPS results were consistent with the ^1H NMR results.

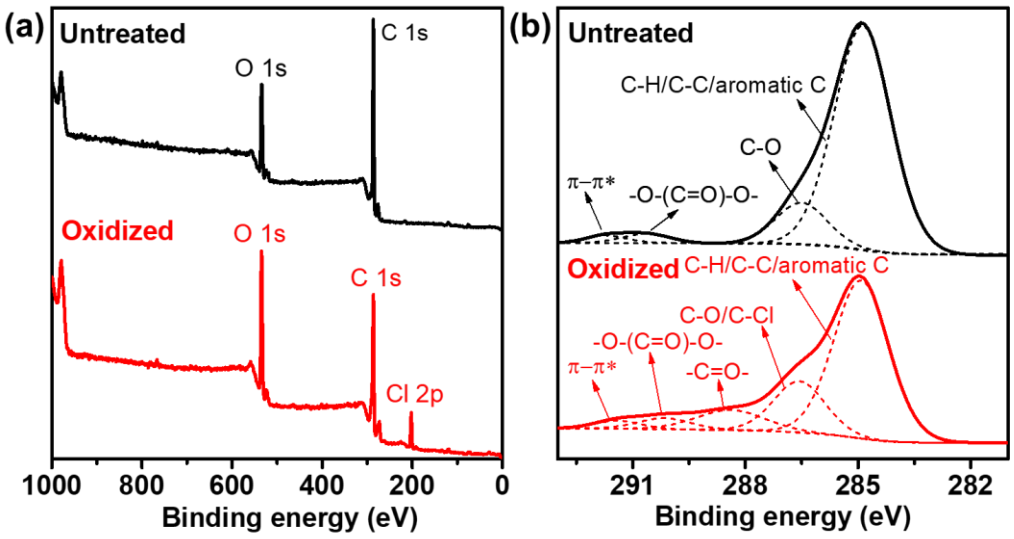

Figure 3-3. (a) X-ray photoelectron spectroscopy (XPS) survey profile and (b) C1s narrow XPS profile of untreated polycarbonate (PC) film and **oxidized PC** surface. Here, **oxidized PC** denotes PC film oxidized using light-activated $ClO_2^{\bullet}$ at 25 °C for 10 min.

The oxidation depth was also determined by the XPS and **oxidized PC** surface were etched by the Ar^+ gas cluster ion while measuring the XPS. The result showed that the oxidation

depth of **oxidized PC** is about 126 nm which indicated the oxidation of PC film surface occurred at nanometer level. The durability of the PC film oxidized by this method in our study was also investigated. The amounts of oxygen and polar functional groups on the surface were determined by XPS 4 months after oxidation. Only a slight decrease was observed in the oxygen amount ratio (from 25.04% to 24.04%) and polar functional groups (taking carboxylic groups as an example: from 4.24% to 4.04%). This result indicated oxidation retarded the rotation and migration of polar functional groups.

In comparison with PP (Chapter 1), the amount ratio of the introduced oxygen and oxygen-containing ratio on the PC film surface is much lower under the same oxidation conditions, which indicated the reactivity of PC is lower than PP. PP is a simple alkane with methyl groups in the side chains. However, PC has an oxygen containing structure, and the aromatic and quaternary carbons exist in its main chain. The lower reactivity of PC may result from lower ratio of carbon of methyl groups in the chemical structure and the different possible reaction mechanisms.

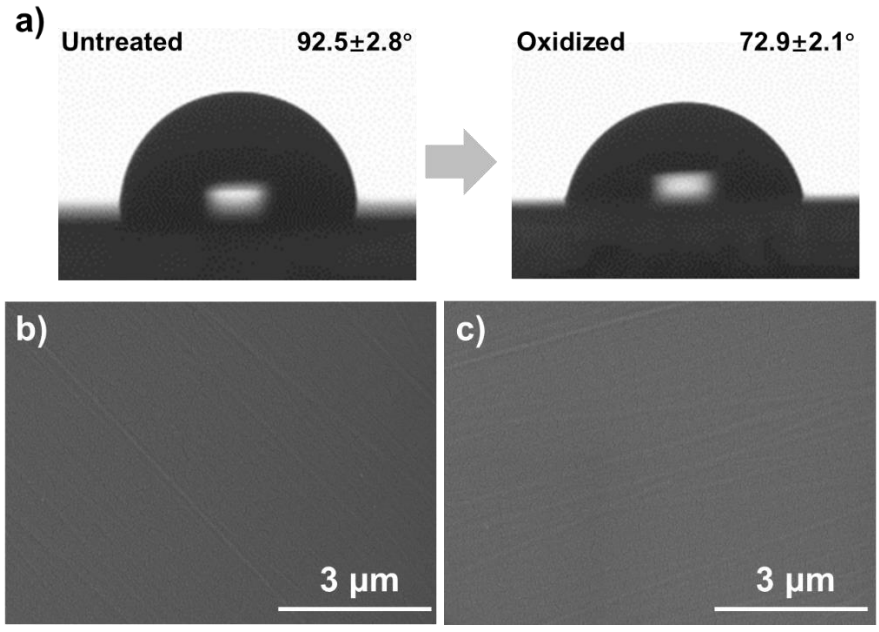

Figure 3-4. (a) Photographs of water contact angles of untreated polycarbonate (PC) film and **oxidized PC** surfaces. Scanning electron micrographs of (b) untreated PC film and (c) **oxidized PC** surfaces. Here, **oxidized PC** denotes PC film oxidized using light-activated $ClO_2^{\bullet}$ at 25 °C for 10 min.

Water contact angle measurements were performed to assess the hydrophilicity of the PC film surface before and after surface oxidation (**Figure 3-4**a). The contact angle of the untreated PC film was 92.5±2.8° and that of **oxidized PC** was decreased to 72.9±2.1°. These results revealed that the hydrophilicity of the PC film surface was improved *via* oxidation. The surface morphologies of untreated PC and **oxidized PC** were observed using SEM. Both film surfaces were smooth (**Figures 3-4**b and c). Besides, the surface roughness was determined by the AFM measurement (**Figure 3-5**). The arithmetical mean deviation of roughness (Ra) of the untreated PC film surface and the **oxidized PC** surface were determined to be 2.208 nm and 1.573 nm, respectively, which indicated that both surface roughness values had no significant difference and both the untreated PC film and the **oxidized PC** possessed smooth surface. Thus, smooth PC film surfaces were provided for the subsequent electroless plating. These results demonstrated that the surface of the PC film was not destroyed during the oxidation reaction performed under UV irradiation, and the surface modifications of the PC films only involved the addition of chemical bonds. In addition, the improvement of the wettability of the PC film surface mainly resulted from the introduction of the surface polar functional groups.

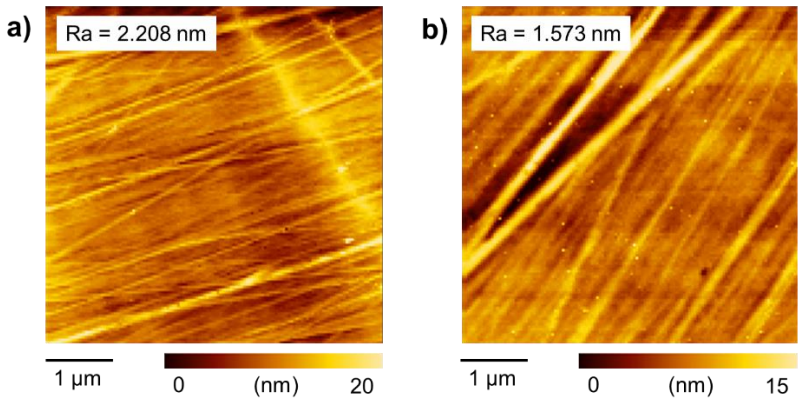

Figure 3-5 Atomic force microscopic (AFM) images of (a) untreated PC film surface; (b) **oxidized PC** surface (Ra: the arithmetical mean deviation of roughness).

Effects of oxidation conditions

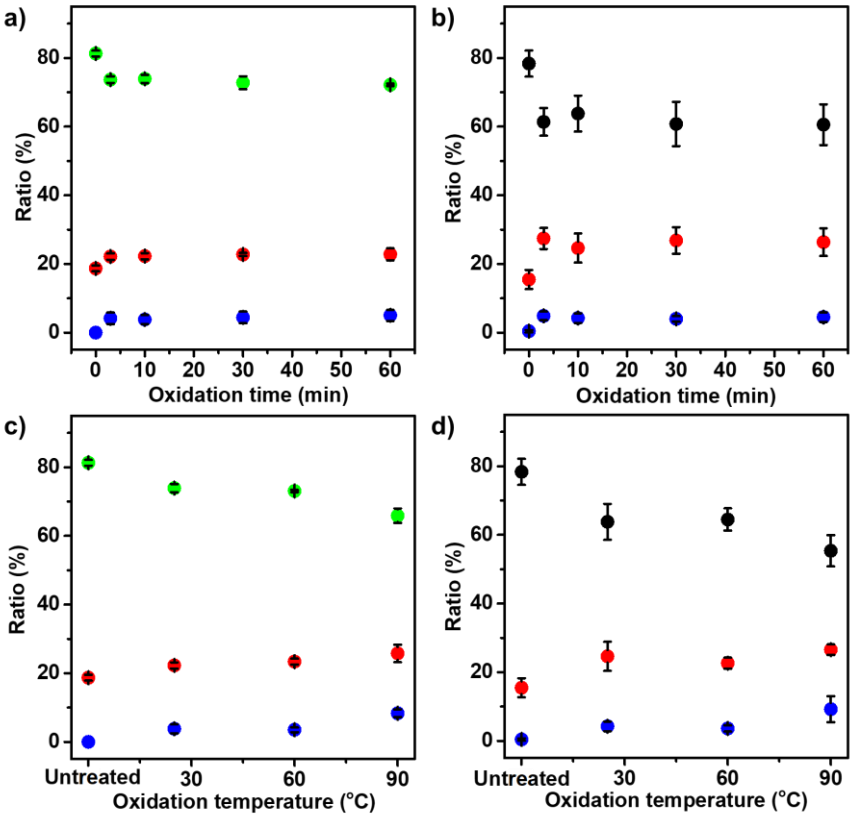

Figure 3-6. Relationship between oxidation temperature and chemical composition of PC film surface calculated using (a) the XPS survey profile (green: C, red: O, blue: Cl) and (b) C1s narrow XPS profile (black: aromatic/aliphatic C, red: C–O/C–Cl, blue: O–C=O) of the PC film surfaces. Relationship between oxidation time and chemical composition of polycarbonate (PC) film surface calculated using (c) the X-ray photoelectron spectroscopy (XPS) survey profile (green: C, red: O, blue: Cl) and (d) C1s narrow XPS profile (black: aromatic/aliphatic C, red: C–O/C–Cl, blue: O–C=O) of the PC film surfaces. Three independent experiments were preformed to obtain the standard deviations.

The effects of oxidation time and temperature on the chemical composition and surface wettability of the PC films were investigated. The PC films were oxidized for different time at 25 °C. The surface chemical compositions after oxidation for different time are presented in **Figures 3-6**a and b. The ratio of O and polar functional groups on the PC film surfaces were increased after oxidation; however, they did not increase with increasing oxidation time. These results indicated that oxidation occurred rapidly and finished fast, which is beneficial for

industrial use. Furthermore, the water contact angles of the PC film surfaces oxidized for different time were almost the same (**Table 3-1**), which was consistent with the XPS results. The SEM images revealed that the surfaces of the PC films oxidized at 25 °C for 10 and 60 min were smooth (**Figures 3-7**a and b), which indicated that the oxidation time did not affect the surface morphology. Thus, the optimal oxidation time was determined to be 10 min.

The effect of oxidation temperature on the chemical composition and surface wettability of the PC films was also investigated. The surface chemical compositions after oxidation for 10 min at different temperatures are illustrated in **Figures 3-6**c and d. As the oxidation temperature increased, the ratios of O and polar groups on the PC film surface increased. SEM images (**Figure 3-7**c and d) were also analyzed to investigate the differences between the morphologies of the PC film surfaces oxidized at different temperatures. The results revealed that the PC film surface chemical structure was destroyed and reorganization occurred at high oxidation temperatures. The increase in the ratios of O and polar groups were attributed to surface damage, which promoted the oxidation at the PC film deeper surfaces.

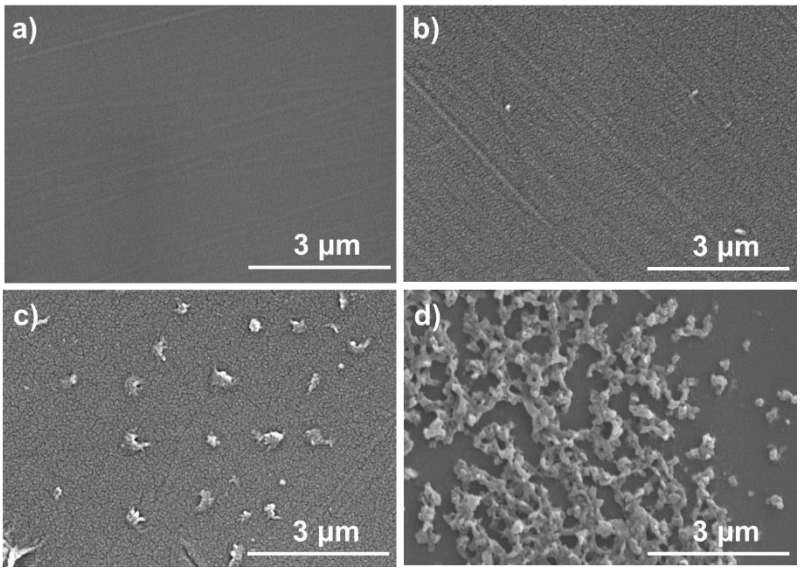

Figure 3-7. Scanning electron micrographs of polycarbonate film surfaces oxidized (a) at 25 °C for 10 min, (b) at 25 °C for 60 min, (c) at 60 °C for 10 min, and (d) at 90 °C for 10 min.

Table 3-1. Water contact angles of the polycarbonate films surface oxidized under different conditions.

Oxidation conditions	untreated	25 °C				60°C	90°C
		3 min	10 min	30 min	60 min	10 min	10 min
Water contact angles (°)	92.5±2.8	74.3 ±1.0	76.8 ±0.7	76.4 ±1.4	76.9 ±2.2	74.7 ±1.8	74.6 ±3.2

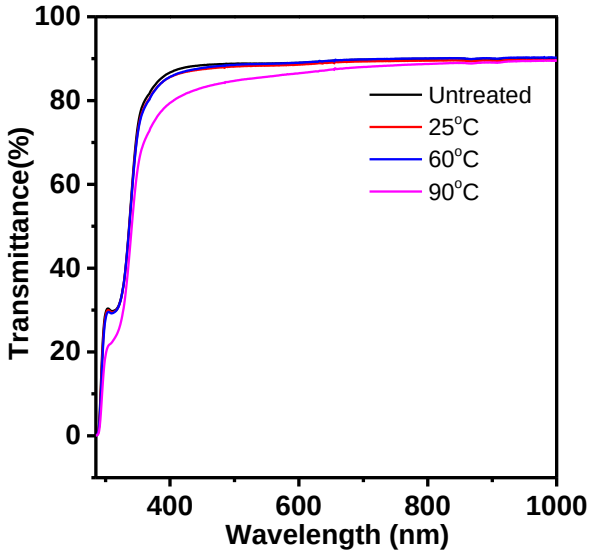

Figure 3-8. Transmittance curves of untreated polycarbonate (PC) plate and PC plate oxidized for 10 min at different temperatures.

Transmittance is a key property for the applications of PC. Researchers have established that the transmittance of PC is affected by the preliminary physical and physical-chemical modifications[19]. The surface damage of the PC film oxidized at elevated temperatures is shown in the SEM images (**Figures 3-7**c and d); the transmittances of an untreated PC plate and PC plate oxidized for 10 min at different temperatures were measured using UV–vis spectroscopy (**Figure 3-8**). The transmittances of the untreated PC plate and PC plates oxidized at 25 and 60 °C for 10 min were similar. However, the transmittance of the PC plate oxidized at 90 °C for 10 min was lower than those of the previously mentioned samples. Moreover, a highly transparency plate should also have a low haze value. The haze value was also determined by

a haze meter and calculated according to **Equation 1**, where T.T. and P.T. indicate the total transmissivity and parallel transmissivity, respectively.

$$\text{Haze} = \frac{T.T - P.T}{T.T} \times 100\% \qquad (1)$$

The results were shown in the **Table 3-2.** The haze values of the untreated PC plate and the PC plate oxidized at 25 °C for 10 min were determined to be 0.11 % and 0.12 %, respectively, while the PC plate oxidized at 60 °C and 90 °C for 10 min have higher haze values of 1.23 % and 8.59 %, respectively. These results were consistent with the SEM results and indicated that the decrease in transmittance and increase in haze values at high oxidation temperatures were attributed to surface damage. Consequently, the optimal oxidation time and temperature were determined to be 10 min and 25 °C, respectively.

Table 3-2. Haze values of untreated polycarbonate (PC) plate and PC plate oxidized for 10 min at different temperatures.

Oxidation conditions	Haze value (%)	T.T (%)	P.T (%)
untreated	0.11	89.33	89.23
25 °C for 10 min	0.12	89.44	89.33
60 °C for 10 min	1.23	89.51	88.40
90 °C for 10 min	8.95	89.57	81.87

In addition, when PC is used in outdoor under the UV of sunlight, photo-oxidation and photo-Fries rearrangement always occur and PC starts to show losses in mechanical properties and changes in optical properties, which means UV irradiation causes the photodegradation of PC materials, so the practical use of UV irradiation is limited.[23,24] Thus, the effect of the UV irradiation on the PC film surface should be investigated. In the chapter 1, UV was only required for the activation of $ClO_2^{\bullet}$ but not for the PP surface oxidation process. A special setup was designed to perform the oxidation of PC film surfaces in the absence of UV light irradiation on the PC film surface. In this oxidation process, UV irradiation on the PC film was prevented by an aluminum sheet and the PC film surface was only exposed to the UV-activated $ClO_2^{\bullet}$. XPS measurements were performed to determine the chemical composition of the surfaces of oxidized PC films (**Table 3-3**), and the results revealed that O-containing groups were

incorporated into the PC films surface after oxidation using UV-activated $ClO_2^{\bullet}$ when the PC film surfaces were not irradiated with UV light. Furthermore, according to the results of the investigation on the effects of the oxidation conditions on the chemical composition of the PC film surfaces, the rate of the oxidation of the PC film surface in the absence of UV irradiation on the PC films surfaces was lower than that of the oxidation of the PC film surface under UV irradiation. Furthermore, the PC film surface was not oxidized when it was only irradiated by UV without using UV-activated $ClO_2^{\bullet}$ as the oxidant. These results indicated that UV irradiation was only required for the activation of $ClO_2^{\bullet}$ and was not necessary for the oxidation of the PC film surface, which could modify PC materials with complex geometric shapes.

Table 3-3. Chemical composition calculated from the X-ray photoelectron spectroscopy measurement of the polycarbonate films surface oxidized under different conditions in the absence of UV irradiation on the polycarbonate films.

Oxidation conditions (absence of UV on surface)	Atomic ratio (%)					
	C	O	Cl	Aromatic /aliphatic C	C-O/C-Cl	O-C=O
25°C for 3 min	80.71	18.57	0.73	66.23	23.73	1.09
25°C for 10 min	77.43	20.46	2.11	63.69	24.44	3.65
25°C for 30 min	71.66	23.97	4.36	59.14	25.84	6.44
60°C for 10 min	71.69	23.37	4.94	57.02	27.45	6.32
90°C for 10 min	67.18	23.00	9.82	56.45	25.46	8.33

Electroless plating of surface-modified PC films

The incorporation of polar functional groups into the surface of polymers *via* oxidation is beneficial for the adhesion of polymers to metal materials. Among the adhesion techniques, electroless plating is an important metallization approach that is widely used in many fields including the fabrication of printed circuits in microelectronics and decorative coating in general manufacturing. To demonstrate that polar groups were incorporated on the PC film surface, both the untreated PC film and **oxidized PC** were subjected to electroless plating using Cu and Ni. After electroless plating, the adhesion of the metal layer to the surface of the PC films was tested using the cross-type Scotch tape test according to the ASTM (D3359-09)

standard (**Figure 3-9**). Both the untreated PC film and **oxidized PC** were completely covered by a thin Cu layer (about 60 nm, **Figure 3-10**b) after electroless plating. After the Scotch tape test, the Cu layer on the untreated PC film was completely removed (**Figure 3-9**a), whereas the Cu layer on the **oxidized PC** sample was not. According to the ASTM standard (5B: The edges of the cuts are completely smooth and none of the squares of the lattice is detached; 4B: Small flakes of the coating are detached at intersections and less than 5% of the area is affected; 3B: Small flakes of the coating are detached along edges and at intersections of cuts and the area affected is 5 to 15% of the lattice; 2B: The coating has flaked along the edges and on parts of the squares and the area affected is 15 to 35% of the lattice; 1B: The coating has flaked along the edges of cuts in large ribbons and whole squares have detached. the area affected is 35 to 65% of the lattice; 0B: Flaking and detachment are worse than 1B), **oxidized PC** showed the adhesion value of 4B while the untreated PC film showed the adhesion value of 0B, which indicated that strong adhesion was achieved between the Cu layer and **oxidized PC**. The Ni electroless plating experiment led to identical results.

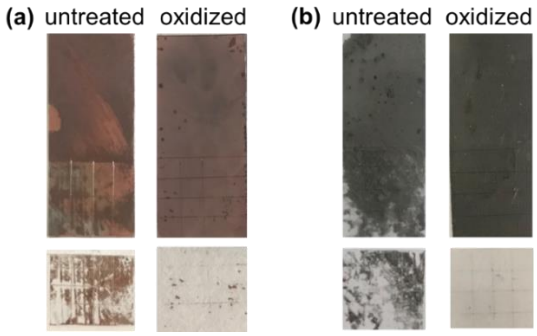

Figure 3-9. Photographs of (a) Cu electroless-plated and (b) Ni electroless-plated polycarbonate (PC) films after the Scotch tape test. Left: untreated PC, Right: **oxidized PC.** The upper rectangular and lower square specimens represent the PC films and the tapes, respectively. Here, **oxidized PC** denotes PC film oxidized using light-activated $ClO_2^{\bullet}$ at 25 °C for 10 min.

Furthermore, the Pd^{2+} (catalyst for electroless plating) amount on the PC film surface before plating and after catalyst-loading was determined using XPS (**Figure 3-11**). The amount of Pd^{2+} attached to the **oxidized PC** surface was higher than that attached to the untreated PC

film surface for both the Cu and Ni electroless plating samples. The improvement of the Pd^{2+} adhesion *via* the induced polar groups was beneficial for the good adhesion between the **oxidized PC** and metal layer.

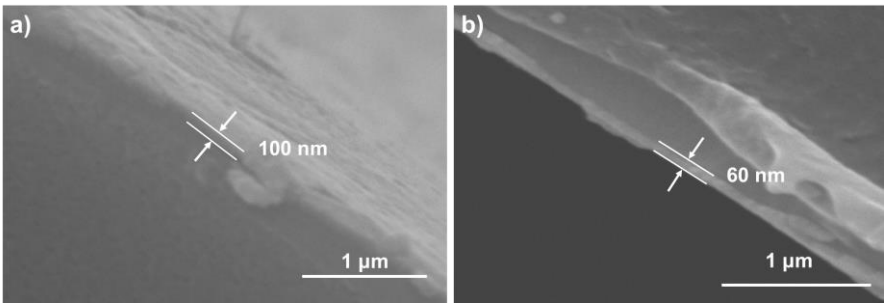

Figure 3-10. The SEM images of the cross sections of (a) Ni and (b) Cu films coated by electroless plating.

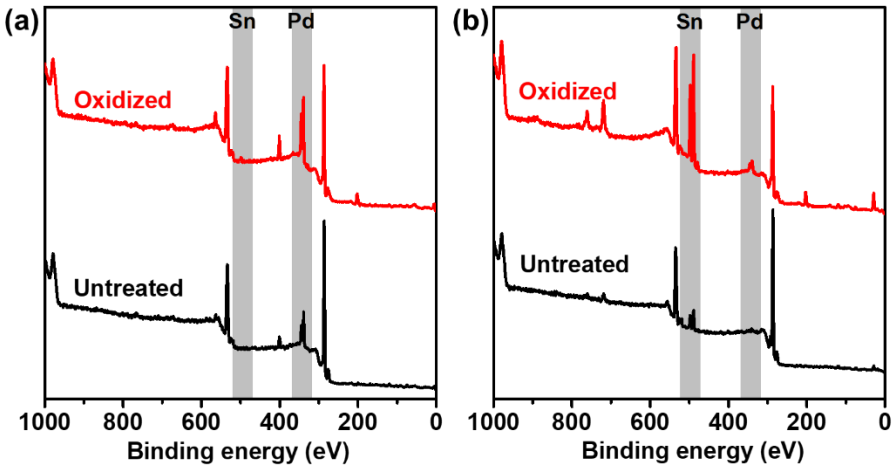

Figure 3-11. X-ray photoelectron spectroscopy survey profile of the untreated PC films and **oxidized PC** surface after catalyst-loading process for electroless plating of (a) Cu and (b) Ni.

3.4 Conclusion

In this chapter, the PC film surface was modified successfully *via* oxidation using light-activated $ClO_2^{\bullet}$ under mild conditions. The chemical composition of the surface was determined using ^{1}H-NMR and XPS, and the results confirmed that polar groups, such as carboxyl, aldehyde, and hydroxyl, were incorporated on the PC film surface. The hydrophilicity of the PC film surface was also analyzed using water contact angle

measurements, and it was determined that surface oxidation improved the hydrophilicity of the typically hydrophobic PC film surface. Furthermore, it was demonstrated that direct light-irradiation on the PC film surface was not required during the surface oxidation process, and eliminating the UV irradiation could prevent the photo-degradation of PC materials. Moreover, the optimal oxidation conditions were determined to be 10 min and 25 °C, which demonstrated that the reaction was complete under these mild conditions. Lastly, after they underwent surface oxidation modification, PC films were subjected to Cu and Ni electroless plating. This study contributed to the development of surface modification technology for PC materials. The oxygenated PC film surface allows further modification with various organic compounds *via* reactions with the induced polar groups on the surface, which could expand the applications of PC materials.

3.5 References

1. V. VanDelinder, D. R. Wheeler, L. J. Small, M. T. Brumbach, E. D. Spoerke, I. Henderson and G. D. Bachand, *ACS Appl. Mater. Interfaces*, 2015, **7**, 5643–5649.
2. A. Qureshi, S. Shah, S. Pelagade, N. L. Singh, S. Mukherjee, A. Tripathi, U. P. Despande and T. Shripathi, *J. Phys. Conf. Ser.*, 2010, **208**, 012108.
3. P. Pedrosa, J. M. Chappé, C. Fonseca, A. V. Machado, J. M. Nóbrega and F. Vaz, *Plasma Process. Polym.* 2010, **7**, 676–686.
4. Y. Liu, D. Ganser, A. Schneider, R. Liu, P. Grodzinski and N. Kroutchinina, *Analysis. Anal. Chem.*, 2001, **73**, 4196–4201.
5. E. A. Soliman, A. Samir, A. M. A. Hassan, A. S. Mohy-Eldin and G. A. El-Naim, *Open J. Synth. Theory Appl.*, 2014, **3**, 27–36.
6. J. E. Biles, T. P. McNeal, T. H. Begley and H. C. Hollifield, *J. Agric. Food Chem.*, 1997, **45**, 3541–3544.
7. R. O. F. Verkuijlen, M. H. A. Van Dongen, A. A. E. Stevens, J. Van Geldrop and J. P. C. Bernards, *Appl. Surf. Sci.*, 2014, **290**, 381–387.

8. C. B. Mello, K. G. Kostov, M. MacHida, L. R. O. De Oliveira Hein and K. A. De Campos, *IEEE Trans. Plasma Sci.* 2012, **40**, 2800–2805.

9. N. Arias and F. Jaramillo, *Appl. Surf. Sci.* 2019, **505**, 144596.

10. M. Šíra, D. Trunec, P. St'ahel, V. Buršíková and Z. Navrátil, *J. Phys. D. Appl. Phys.* 2008, **41**, 015205.

11. T. G. Shikova, A. A. Ovtsyn and S. A. Smirnov, *High Energy Chem.*, 2019, **53**, 326–330.

12. L. Zajíčková, V. Buršíková, V. Peřina, A. Macková, D. Subedi, J. Janča and S. Smirnov, *Surf. Coatings Technol.*, 2001, **142**, 449–454.

13. T. Yoshida and M. A. Okoshi, *Surfaces and Interfaces*, 2019, **17**, 100373.

14. G. Chen, Z. K. Wang, H. Y. Zheng, A. M. Thwe and Y. C. Lam, *Opt. Laser Technol.*, 2019, **115**, 316–324.

15. S. K. Koh, S. K. Song, W. K. Choi, H. J. Jung, S. N. Han, *J. Mater. Res.*, 1995, **10**, 2390–2394.

16. A. M. A. Reheem, M. I. A. A. Maksoud and A. H. Ashour, *Radiat. Phys. Chem.*, 2016, **125**, 171–175.

17. R. Nathawat, A. Kumar, V. Kulshrestha, M. Singh, V. Ganesan, D. M. Phase and Y. K. Vijay, *Appl. Surf. Sci.*, 2007, **253**, 5985–5991.

18. A. S. Bhurke, P. A. Askeland and L. T. Drzal, *J. Adhes.*, 2007, **83**, 43–66.

19. H. Yaghoubi and N. Taghavinia, *Appl. Surf. Sci.*, 2011, **257**, 9836–9839.

20. W.J. Brennan, W.J. Feast, H.S. Munro and S.A. Walker, *Polymer (Guildf)*, 1991, **32**, 1527–1530.

21. K. Ohkubo, H. Asahara and T. Inoue, *Chem. Commun.*, 2019, **55**, 4723–4726.

22. A. Rivaton, D. Sallet and J. Lemaire, *Polym. Photochem.*, 1983, **3**, 463–481.

23. M. Diepens and P. Gijsman, *Polym. Degrad. Stab.*, 2007, **92**, 397–406.

24. G. F. Tjandraatmadja, L. S. Burn and M. C. Jollands, *Polym. Degrad. Stab.*, 2002, **78**, 435–448.

Concluding Remarks

In this doctoral thesis, novel modification method *via* oxidation using the light-activated $ClO_2^{\bullet}$ was developed for the surface modification of plastics. As mentioned in this thesis, due to the surface low energy of the plastics, surface modifications are required to expand the range of their applications. Although the researchers have made much effort to investigate the plastics surface modification methods, such as physical treatments of plasma, laser, etc., wet medical treatment and patterning, there is still high demand of strategy for the efficient surface modification method without change in bulk properties. The results obtained in this thesis about plastics surface modification *via* oxidation using the light-activated $ClO_2^{\bullet}$ are summarized as follows.

In chapter 1, the surface modification of PP *via* oxidation using the light-activated $ClO_2^{\bullet}$ was achieved. The oxygen and oxygen-containing groups such as the hydroxyl and carbonyl groups were introduced onto film surface after surface oxidation. The improvement of surface hydrophilicity was also observed. The adhesion enhancement of PP film with Al plate after oxidation without any adhesives was also demonstrated. Although the number of functional groups introduced to the outermost surface did not depend on the reaction temperature, a positive correlation between the oxidation depth (oxidation temperature) of PP and the adhesive strength was exhibited. The electroless metal plating on PP was achieved as well. Furthermore, the UV irradiation was required only for the activation of $ClO_2^{\bullet}$ gas but not for surface modification process, which resulted in the well metal plating on the PP mesh film. This oxidation was confirmed to be an effective approach for the PP surface modification.

In chapter 2, oxidation via light-activated $ClO_2^{\bullet}$ was conducted on the ABS resin plate surface and demonstrated to be useful for its surface modification. An increase in the amount of surface polar functional groups resulting from the incorporation of oxygen-containing groups into ABS resin surface was confirmed. Improvement in the surface hydrophilicity of ABS resin was also observed after oxidation. The oxidation appearing in the C=C of butadiene in the ABS resin was confirmed by ^{1}H NMR spectroscopy. The effect of oxidation conditions

was studied to determine that the optimal oxidation time and temperature was 10 min and 25 ℃, respectively. Besides, after surface oxidation, the ABS resin plate exhibited good adhesion to the metal layer after electroless metal plating. Basing on the achievement of surface oxidation *via* light-activated $ClO_2^{\bullet}$ without UV irradiation on the ABS resin surface, ABS resins with complex shape were also successfully electroless plated. This method could be applied as an effective alternative pretreatment for the electroless plating of ABS resin instead of the traditional methods.

In chapter 3, light-activated $ClO_2^{\bullet}$ was used as an oxidizing agent for PC oxidation by light irradiation under mild conditions. Polar groups like carboxyl, aldehyde, and hydroxyl were added to the surface of the PC films without causing surface damage. The PC film surface hydrophilicity and adhesion with metal layer obtained from electroless plating were improved after surface oxidation, and the specific character of transmittance of the PC films did not decrease. Moreover, the investigation of oxidation conditions indicated that the surface chemical compositions did not change with the increase in oxidation time, while the high temperature caused the surface damage. So the oxidation under a mild ambient conditions is effective for PC films modification.

In conclusion, the three types of plastics with different kinds of chemical structures described in this thesis were successfully modified by the oxidation and exhibited good adhesion properties with metal materials. This oxidation can be conducted in the atmospheric environment without high cost, high energy and surface damage. Also, the oxygen groups on the surface were stable for long time. The $ClO_2^{\bullet}$ gas used in this oxidation was flowable without wet environment, which is beneficial to metal plating on the polymers with the complex shape. This study provided a new strategy for the surface modification of plastics using the clean and energy-saving light-activated $ClO_2^{\bullet}$ oxidation method. The oxidized plastics surface allows further modification with various organic compounds *via* reaction with the functional groups on the surface, which may have significant implications in synthetic polymer chemistry.

List of Publications

1. Polymer Surface Oxidation by Light-Activated Chlorine Dioxide Radical for Metal−Plastics Adhesion
   Yankun Jia, Jiaxin Chen, Haruyasu Asahara*, Taka-Aki Asoh*, and Hiroshi Uyama
   ACS Appl. Polym. Mater., 2019, 1(12), 3452−3458.
   DOI: 10.1021/acsapm.9b00871

2. Photooxidation of the ABS Resin Surface for Electroless Metal Plating
   Yankun Jia, Jiaxin Chen, Haruyasu Asahara, Yu-I Hsu*, Taka-Aki Asoh and Hiroshi Uyama*
   Polymer, 2020, 200, 122592.
   DOI: 10.1016/j.polymer.2020.

3. Surface Modification of Polycarbonate Using the Light-Activated Chlorine Dioxide Radical
   Yankun Jia, Haruyasu Asahara, Yu-I Hsu*, Taka-Aki Asoh and Hiroshi Uyama*
   Applied Surface Science, 2020, 530, 147202.
   DOI: 10.1016/j.apsusc.2020.147202.

Acknowledgments

This study was carried out from 2017 to 2020 at the Department of Applied Chemistry, Graduate School of Engineering, Osaka University. During this fantastic experience in the doctoral 3 years, I have received a lot of invaluable assistance from all people around me. Their support and advices contribute to the accomplishment of the thesis.

First and foremost, I would like to express my deepest gratitude to my supervisor, Prof. Hiroshi Uyama, for his continuous guidance and discussion on my research, and his kind-hearted encouragement as well. I also sincerely thank him for providing 4 opportunities to attend the academic conferences including the internal and international ones, by which my views were broadened, my knowledge was expanded and my ability was improved. His keen and vigorous academic observations enlighten me in my future study and career.

I am profoundly grateful to Assoc. Prof. Taka-aki Asoh, for his suggestions and inspirations to improve the quality of my research. His novel insights and knowledge sharing promoted my thesis' accomplishment. I also thank him for his suggestions and revision about the slides art to make it easier to understand.

I appreciate Assist. Prof. Yu-I Hsu for her discussions and advices about my subject at any time and the knowledge sharing. I also deeply thank her for the manuscripts revising, inspirations and experience sharing. Without her support, my doctoral thesis cannot be finished smoothly.

I am especially grateful to Assoc. Prof. Haruyasu Asahara for his advices about the experiments, manuscripts revising, and encouragement. Without his sharing of the basic knowledge about the data analysis, oxidation theory and polymer surface modification, I cannot deeply understand these methods and experiments.

I also appreciate the help from Dr. Hitoshi Haneoka for the XPS measurement and analysis.

I also would like to express my gratitude to Mr. Koji Kita and Mr. Junji Yoshikawa of Okuno Chemical Industry for metal plating reagent and advices.

I wish to appreciate the kind help and warm-hearted support from Ms. Yoko Uenishi and Ms. Tomoko Shimizu.

I am very thankful to the past and present fellow labmates in Uyama Lab: Dr. Qidong Wang, Dr. Yu Shu, Dr. Zhaohang Yang, Dr. Masatoshi Kato, Ms. Lulu Huang, Mr. Weiting Wu, Mr. Chen Qian, Mr. Zhengtian Xie, Mr. Shunsuke Mizuno, Mr. Toshiki Tamiya, Ms. Hanyu Wen, Ms. Yanting Lyu, Mr. Akihide Sugawara, Mr. Mark Adam Malaluan Ferry, Ms. Zeying Cao, Ms. Jiaxin Chen, etc. for their kind-hearted help both in my research and daily life.

The financial support from Otsuka Toshimi Scholarship Foundation for my academic study and my stay in Japan is greatly appreciated.

Last but not least, I would like to express appreciation to my parents Fuyi Jia and Shuzhen Ma, and my husband, Shijun Zhang for their endless support and love throughout my life. The warm encouragement from my family motivates me to persist in my research and study.

July 2020

Yankun Jia